

---

Masters Theses

Student Theses and Dissertations

---

1971

## A comparison of computer codes for fast neutron dosimetry by the foil technique

Jau Wen Chen

Follow this and additional works at: [https://scholarsmine.mst.edu/masters\\_theses](https://scholarsmine.mst.edu/masters_theses)

 Part of the [Nuclear Engineering Commons](#)

Department: Mining and Nuclear Engineering

---

### Recommended Citation

Chen, Jau Wen, "A comparison of computer codes for fast neutron dosimetry by the foil technique" (1971). *Masters Theses*. 6706.

[https://scholarsmine.mst.edu/masters\\_theses/6706](https://scholarsmine.mst.edu/masters_theses/6706)

This thesis is brought to you by Scholars' Mine, a service of the Curtis Laws Wilson Library at Missouri University of Science and Technology. This work is protected by U. S. Copyright Law. Unauthorized use including reproduction for redistribution requires the permission of the copyright holder. For more information, please contact [scholarsmine@mst.edu](mailto:scholarsmine@mst.edu).

A COMPARISON OF COMPUTER CODES FOR FAST NEUTRON DOSIMETRY  
BY THE FOIL TECHNIQUE

BY

JAU WEN CHEN, 1944-

A THESIS

Presented to the Faculty of the Graduate School of the

UNIVERSITY OF MISSOURI-ROLLA

In Partial Fulfillment of the Requirements for the Degree

MASTER OF SCIENCE IN NUCLEAR ENGINEERING

1971

Approved by

D. Ray Edwards (Advisor)      James K. Byers  
Albert E. Boston

## ABSTRACT

A comparison of the major codes currently used for fast neutron dosimetry based on the foil technique has been made. These codes are SAND II, SPECTRA and RDMM. The comparison is based upon the deviation of calculated-from-measured activities, the input data decks, the obtained information, and the computer time required.

Four sets of data were used to be compared upon the above four viewpoints, the conclusion reached is that the SPECTRA computer code is the most satisfactory for the UMR Reactor fast neutron spectrum.

## ACKNOWLEDGMENTS

The author wishes to thank Dr. D. Ray Edwards, Director of the University of Missouri - Rolla Nuclear Reactor Facility, for suggesting this project and assisting in its completion.

He is also grateful to Mr. Michael L. Martin, systems analyst in the Computer Science Department, for his assistance when problems arose in the computer program involved in this thesis.

Finally, the author wants to thank Bryce Shriver very much for the cooperating to obtain the UMRR 5-foil activity data.

## TABLE OF CONTENTS

	Page
ABSTRACT .....	ii
ACKNOWLEDGEMENT .....	iii
TABLE OF CONTENTS	
LIST OF FIGURES .....	vi
LIST OF TABLES .....	vii
I. INTRODUCTION .....	1
II. STATEMENT OF THE PROBLEM .....	3
III. REVIEW OF LITERATURE .....	4
A. SAND II CODE .....	4
B. RDMM CODE .....	11
C. SPECTRA CODE .....	16
IV. RESULTS AND DISCUSSION .....	21
A. COMPUTER TIME REQUIRED .....	22
B. CALCULATED-TO-MEASURED ACTIVITY RATIOS ..	22
C. COMPLEXITY OF INPUT DATA .....	24
D. OUTPUT .....	24
V. CONCLUSIONS .....	39
VI. RECOMMENDATIONS .....	40
A. SAND II CODE .....	40
B. RDMM CODE .....	41
C. SPECTRA CODE .....	41
APPENDICES .....	42
A. DATA FORMAT USED IN COMPUTER CODES .....	42
A.1. SAND II CODE .....	42

## TABLE OF CONTENTS (continue)

	Page
A.2. RDMM CODE .....	44
A.3. SPECTRA CODE .....	45
B. RELATIONS FOR ACTIVITIES IN COMPUTER CODES .....	53
C. CROSS-SECTION INFORMATION USED IN COMPUTER CODES .....	54
D. RECOMMENDATIONS IN USING COMPUTER CODES ..	75
D.1. SAND II CODE .....	75
D.2. RDMM CODE .....	75
D.3. SPECTRA CODE .....	76
E. CURRENTLY OUTPUT DESCRIPTIONS .....	77
E.1. SAND II CODE .....	77
E.2. RDMM CODE .....	78
E.3. SPECTRA CODE .....	79
F. CHARACTERISTICS OF THE UMR REACTOR .....	81
BIBLIOGRAPHY .....	85
VITA .....	86

## LIST OF FIGURES

Figures	Page
1. Neutron differential spectrum for 10 foils .....	31
2. Neutron integral spectrum for 10 foils .....	32
3. Neutron differential spectrum for 5 foils .....	33
4. Neutron integral spectrum for 5 foils .....	34
5. Neutron differential spectrum for 7 foils, no version .....	35
6. Neutron integral spectrum for 7 foils, no version .....	36
7. Neutron differential spectrum for 7 foils, version III .....	37
8. Neutron integral spectrum for 7 foils, version III .....	38
C.1. The cross-section as a function of neutron energy for $\text{Al}^{27}(\text{n},\text{He})\text{Na}^{24}$ , $\text{Al}^{27}(\text{n},\text{p})\text{Mg}^{27}$ , $\text{Cu}^{63}(\text{n},\text{G})\text{Cu}^{64}$ .....	57
C.2. The cross-section as a function of neutron energy for $\text{Fe}^{54}(\text{n},\text{p})\text{Mn}^{54}$ , $\text{Fe}^{56}(\text{n},\text{p})\text{Mn}^{56}$ , $\text{In}^{115}(\text{n},\text{n})\text{In}^{115\text{m}}$ .....	58
C.3. The cross-section as a function of neutron energy for $\text{Au}^{197}(\text{n},\text{G})\text{Au}^{198}$ , $\text{Mg}^{24}(\text{n},\text{p})\text{Na}^{24}$ , $\text{Ni}^{58}(\text{n},\text{p})\text{Co}^{58}$ .....	59
C.4. The cross-section as a function of neutron energy for $\text{Th}^{232}(\text{n},\text{f})\text{FP}$ , $\text{U}^{235}(\text{n},\text{f})\text{FP}$ , $\text{U}^{238}(\text{n},\text{f})\text{FP}$ .....	60
F.1. Diagram of UMRR Core Loading 31T .....	82

## LIST OF TABLES

Tables	Page
1. Computer Time Required Comparison .....	27
2. Calculated-to-Measured Activity Ratios .....	28
A.1. SAND II Code 5 Foils Data Set .....	47
A.2. RDMM Code 5 Foils Data Set .....	49
A.3. SPECTRA Code 5 Foils Data Set .....	52
C. Library Cross-section .....	61
F. Tabulated Differential Flux at C.3 .....	83



## I. INTRODUCTION

Using threshold detectors for the measurement of fast neutron spectra has been a common practice for many years [1], and the method has been improved many times. These techniques are based upon a determination of the specific activity of a detector and from the activity a deduction is made, through knowing the detector response function, of the neutron flux and/or energy distribution which induced the radioactivity.

In the thermal neutron measurements, the characteristic shape of the neutron environment is known and a measurement with a single detector is sufficient to establish the magnitude of the neutron flux. But, many measurements are necessary in epithermal and fast neutron environments where only a general shape of the energy distribution of the neutrons is known. Thus, in these situations the utilization of several activation detectors with different response functions for neutron activation has seen acceptance and is reliable.

The threshold detector technique has the following advantage [4,8] :

1. the threshold detectors are not sensitive to the high gamma fluxes found in reactors,
2. the activation measurement is easy and not very expensive,
3. the small volume and low macroscopic cross-

section of the detectors minimize flux deformations,

4. no connections with the outside of the reactor are required.

The method of interpretation of the activation is described in Section II, whereas Section III will briefly describe the three major codes currently used in this technique. These codes are SAND II, SPECTRA and RDMM. Section IV describes results and conclusions of the comparison of these codes.

## II. STATEMENT OF THE PROBLEM

Measurements of in-pile fast neutron spectra are often by threshold detector irradiations. The threshold detector technique gives results usually expressed as normalized activation rates,

$$A_i = \int_0^{\infty} \sigma_i(E) \phi(E) dE \quad (1)$$

where  $\sigma_i(E)$  is the energy dependent activity cross-section,  $A_i$  is the reaction rate for a nucleus of the  $i$ 'th isotope, and  $\phi(E)$  n/cm<sup>2</sup>-sec-Mev is the time integrated, energy dependent unknown neutron flux.

Three codes, described in the following section, allow the  $\phi(E)$  determination, and we want to compare the three major codes currently used in this technique.

In order to solve Equation 1 and find the flux spectra, two basic principles are used [8] :

1. the total energy range is divided into energy bands;
2. in each energy band a spectral shape is assumed which is predicted by theoretical considerations and calculations.

The criteria of the comparisons will be based upon several items, such as, the relative deviation, the complexity of input data, the obtained information from the output, and the computer time required.

### III. REVIEW OF LITERATURE

A number of techniques have been suggested for the solution of Equation 1 for the energy dependent neutron flux. The resulting spectra come in many forms:

1. histogram,
2. piecewise linear,
3. series expansion (e.g., power exponential, orthogonal function),
4. combinations of the above with special physical shapes,
5. combinations of the above with weight functions.

Where histogram or piecewise linear representations are obtained, generally no assumptions are made concerning the spectral shape. In the case of series expansions, this may or may not be true. The spectrum always, however, has a shape characteristic of the expansion functions and weighting functions; and special physical shapes always imply some assumptions about the spectral shape.

The major codes currently used, SAND II, SPECTRA and RDMM, will be discussed as follows:

#### A. SAND II CODE [2]

The original version of this code gave spurious structure propagated by the iterative method from differential structure in neutron detector reaction cross-sections.

The iterative algorithm used in the SAND II code can be written as:

$$\phi_j^{(k+1)} = \phi_j^{(k)} \exp(C_j^{(k)}), \quad j=1,2,\dots,m; \quad (2)$$

where

$$C_j^{(k)} = \frac{\sum_{i=1}^n w_{i,j}^{(k)} \ln(A_i/A_i^{(k)})}{\sum_{i=1}^n w_{i,j}^{(k)}}, \quad j=1,2,\dots,m; \quad (3)$$

$$w_{i,j}^{(k)} = A_{i,j}^{(k)} / A_i^{(k)}, \quad j=1,\dots,m; \quad i=1,\dots,n; \quad (4)$$

$$A_{i,j}^{(k)} = \phi_j^{(k)} \sigma_{i,j} (E_{j+1} - E_j), \quad \begin{matrix} j=1,2,\dots,m; \\ i=1,2,\dots,n; \end{matrix} \quad (5)$$

$$A_i^{(k)} = \sum_{j=1}^m A_{i,j}^{(k)}, \quad i=1,2,\dots,n; \quad (6)$$

$\phi_j^{(k)}$  =  $k^{\text{th}}$  iterative differential flux over the  $j^{\text{th}}$  energy interval;

$C_j^{(k)}$  =  $k^{\text{th}}$  iterative flux correction term for the  $j^{\text{th}}$  energy interval;

$A_i$  = measured activity for the  $i^{\text{th}}$  detector reaction (extrapolated to saturation and infinite dilution);

$A_i^{(k)}$  = calculated (saturated, infinite dilute) activity for the  $i^{\text{th}}$  detector reaction, based on the  $k^{\text{th}}$  iterative flux spectrum;

$A_{i,j}^{(k)}$  = that portion of  $A_i^{(k)}$  contributed by neutrons in the  $j^{\text{th}}$  energy interval;

$\sigma_{i,j}$  =  $i^{\text{th}}$  detector reaction cross-section  
(averaged constant) over the  $j^{\text{th}}$  energy  
interval;

$E_j$  = lower energy bound of the  $j^{\text{th}}$  energy  
interval;

$m$  = total number of energy intervals (currently  
620);

$n$  = number of detectors used.

The first attempt to minimize spurious structure was a renormalization of the weighting function to unity quotient of total activity divided by effective range.

That is, Equation 5 was replaced by

$$w_{i,j}^{(k)} = (E_{H,i} - E_{L,i})^{(k)} A_{i,j}^{(k)} / A_i^{(k)},$$

where  $E_{L,i}$  and  $E_{H,i}$  are the 5% and 95% "tail" cutoff energies, respectively, for the  $i^{\text{th}}$  reaction sensitivity. The original normalization effectively gave each reaction measurement equal total effect, in some sense, on the total solution flux; thus the new normalization was intended to make each reaction affect the total flux only in proportion to the relative size of the energy region over which it is sensitive. The effect is to reduce the magnitude of those weighting functions which consist mostly of very large resonance peaks over very narrow energy regions so as to reduce the reflections of these peaks in the solution spectrum.

Second, an attempt was made to find some two-parameter analytical form for use as the weighting function, which would describe the sensitivity distribution of a given reaction by means of first and second moments ( $\mu$  and  $\mu_2$ , respectively). The beta distribution was used. The form is:

$$w(x) = x^a(1-x)^b, \quad 0 \leq x \leq 1,$$

where

$$X = (x-x_L)/(x_H-x_L),$$

$$a = (2M^2 - M_2(M+1))/(M_2 - M^2),$$

$$b = (M - (2-M)M_2)/(M_2 - M^2),$$

$$M = (\mu - x_L)/(x_H - x_L),$$

$$M_2 = (\mu_2 - x_L(2\mu - x_L))/(x_H - x_L)^2,$$

and  $x_L$  and  $x_H$  are suitably chosen lower and upper limits, respectively, for  $x$ .

At last, the method of moving  $k$ -point  $n^{\text{th}}$  degree polynomial least-squares fitting as being both appropriate and convenient was selected. In this method, each tabulated value of a function is replaced by the value of a polynomial of degree  $n$  fitted by standard least-squares techniques to a subrange of  $k$  (odd) points, centered (if possible) at the point being modified. Thus, each smoothed value is obtained from a distinct least-squares polynomials except near each end of the

range of the function being smoothed, where the polynomial fitted to the extreme  $k$  points is used to smooth the extreme  $(k+1)/2$  points. Clearly for any given  $k$ ,  $n=1$  (straight line) provides the most severe smoothing, and for any given  $n$ , smoothing severity increases with increasing  $k$ . Thus, for trial purposes,  $n=1$  was chosen for testing various values of  $k$ . In general,  $k$  is odd, then for least-squares fitting of a straight line to the  $k$  points  $(x_i, y_i)$ ,  $i=j-\frac{k-1}{2}, \dots, j+\frac{k-1}{2}$ . And assume the points are equispaced along the abscissa, that is, for all  $i$ ,  $x_i - x_{i-1} = d$ , and if  $X_i$  is defined by

$$X = \frac{x_i - x_j}{d} = \frac{(i-j)d}{d} = i-j,$$

then let  $i_L$  and  $i_H$  be denoted  $j - \frac{k-1}{2}$  and  $j + \frac{k-1}{2}$ , respectively.

$$\begin{aligned} \sum_{i=i_L}^{i_H} X_i &= \sum_{i=i_L}^{i_H} i - \sum_{i=i_L}^{i_H} j \\ &= \frac{(j+\frac{k-1}{2})(j+\frac{k-1}{2}+1) - (j-\frac{k-1}{2}-1)(j-\frac{k-1}{2})}{2} - kj = 0, \quad (7) \end{aligned}$$

and

$$\begin{aligned} \sum_{i=i_L}^{i_H} X^2 &= \sum_{i=i_L}^{i_H} i^2 - 2j \sum_{i=i_L}^{i_H} i + \sum_{i=i_L}^{i_H} j^2 \\ &= \frac{1}{6} (j+\frac{k-1}{2})(j+\frac{k+1}{2})(2j+k) - (j-\frac{k-1}{2})(j-\frac{k+1}{2})(2j-k) \end{aligned}$$



$$\begin{aligned}
& -j\left(j+\frac{k-1}{2}\right)\left(j+\frac{k+1}{2}\right)-\left(j-\frac{k-1}{2}\right)\left(j-\frac{k+1}{2}\right)+kj^2 \\
& = k(k^2-1)/12. \tag{8}
\end{aligned}$$

Thus, if  $w_X = aX + b$  is fitted to the  $k$  points  $(X_i, y_i)$ , where

$$\begin{aligned}
a &= \frac{k \sum X_i y_i - \sum X_i \sum y_i}{k \sum X_i^2 - \left(\sum X_i\right)^2} = \frac{12 \sum X_i y_i}{k(k^2 - 1)}, \\
b &= \frac{\sum X_i^2 \sum y_i - \sum X_i \sum X_i y_i}{k \sum X_i^2 - \left(\sum X_i\right)^2} = \frac{\sum y_i}{k}. \tag{9}
\end{aligned}$$

where  $i$  from  $j - \frac{k-1}{2}$  to  $j + \frac{k+1}{2}$ .

$$w_{X=X_j} = w_{X=0} = \frac{1}{k} \sum_{i=j-\frac{k-1}{2}}^{j+\frac{k-1}{2}} y_i, \quad j=\frac{k+1}{2}, \dots, m-\frac{k-1}{2}, \tag{10}$$

where  $m$  is the total number of points in the range.

To smooth  $y_j$  for  $j=1, \dots, \frac{k-1}{2}$ , and for  $j=m-\frac{k+1}{2}, \dots, m$ , the straight lines centered about  $(X_{(k+1)/2}, y_{(k+1)/2})$  and  $(X_{m-(k-1)/2}, y_{m-(k-1)/2})$  are used respectively. The resultant smoothing forms are:

$$w_{X=X_j} = \frac{1}{k} \left[ \frac{6(2j-k-1)}{k^2-1} \sum_{i=1}^k \left(i - \frac{k+1}{2}\right) y_i + \sum_{i=1}^k y_i \right]. \quad j=1, \dots, \frac{k-1}{2}; \tag{11}$$

and

$$W_{x=x_j} = \frac{1}{k} \left[ \frac{6(2j-2m+k-1)}{k^2-1} \sum_{i=m-\frac{k-1}{2}}^m \left( i-m+\frac{k-1}{2} \right) y_i + \sum_{i=m-\frac{k-1}{2}}^m y_i \right],$$

$$j=m-\frac{k-3}{2}, \dots, m. \quad (12)$$

The smoothing forms of Eqs. 10 through 12 are based on equidistant abscissa spacing. Since, in the SAND II code, the energy grid is approximately logarithmic between  $10^{-10}$  and 1 Mev, and linearly spaced between 1 and 18 Mev, this smoothing technique provides quasi-semilogarithmic least-squares smoothing below 1 Mev and rigorous linear least-squares smoothing above 1 Mev. Since it restricts the ends of all weighting functions to be linear and the least-squares line could assume negative values in extreme low and high regions, thus the weighting functions are modified by Eqs. 13 through 15 using for smoothing.

$$W_{i,j}^{(k)} = \sum_{l=1}^{l_2} A_{i,l}^{(k)} / (l_2 - l_1 + 1) A_i^{(k)}, \quad \begin{matrix} j=2, \dots, m-1; \\ i=1, \dots, n; \end{matrix} \quad (13)$$

$$\text{where } l_1=1, \quad j=2, \dots, \left( \frac{N_S-1}{2} \right), \quad (13a)$$

$$= j - \left( \frac{N_S-1}{2} \right), \quad j = \left( \frac{N_S+1}{2} \right), \dots, \left( m - \frac{N_S-1}{2} \right), \quad (13b)$$

$$= 2j - m, \quad j = m - \left( \frac{N_S-3}{2} \right), \dots, (m-1), \quad (13c)$$

$$\text{and } l_2=2j-1, \quad j=2, \dots, \left( \frac{N_S-1}{2} \right), \quad (13d)$$

$$= j + \left( \frac{N_S-1}{2} \right), \quad j = \left( \frac{N_S+1}{2} \right), \dots, \left( m - \frac{N_S-1}{2} \right), \quad (13e)$$

$$=m, \quad j = \left( m - \frac{N_S - 3}{2} \right), \dots, (m-1); \quad (13f)$$

$$W_{i,1}^{(k)} = \left( 5A_{i,1}^{(k)} + 2A_{i,2}^{(k)} - A_{i,3}^{(k)} \right) / 6A_i^{(k)}, \quad (14)$$

$$W_{i,m}^{(k)} = \left( 5A_{i,m}^{(k)} + 2A_{i,m-1}^{(k)} - A_{i,m-2}^{(k)} \right) / 6A_i^{(k)}. \quad (15)$$

The influence of the various degree of smoothing, represented by Eqs. 13 through 15, on solution spectra is much as would be expected. The most important observation is that the degree of smoothing (value of  $N_S$ ) is a fairly sensitive function of the particular conditions which apply. It is emphasized that the manual spectral smoothing discussed here is very different from the weighting function smoothing. The spectral smoothing will in general change the values of calculated detector activities and may result in a spectrum which is not an appropriate solution. The weighting function smoothing simply affects the iterative procedure, but in no way affects the accuracy of the activity calculations for the eventual solution spectrum.

## B. RDMM CODE [3]

This code is based on the group of methods known as 'polynomial' and 'orthogonal' methods [4], because

1. it seems to be the most suitable for the neutron spectral description, since it is not restricted to reactor-type spectra.
2. a development is possible that allows inter-

pretation of the activation data, even when the detectors do not have completely linearly independent cross-sections.

The polynomial method uses as the spectral shape a polynomial in energy having as many terms as there are detectors used multiplied by a chosen weighting function. The orthonormal method uses a series expansion of orthonormal functions. Then

$$\phi(E) = W(E) \sum_{k=1}^n a_k \psi_k \quad (16)$$

where

$n$  = number of detectors,

$a_k$  = coefficient constant,

$W(E)$  = weighting function,

$\psi_k(E)$  = system of function.

In fact, by introducing the Equation 16 into 1, one obtains:

$$A_i = \sum_{k=1}^n a_k S_{ik} , \quad i=1, \dots, n; \quad (17)$$

where

$$S_{ik} = \int W(E) \psi_k(E) \sigma_i(E) dE \quad (18)$$

The following conditions are implicit in the above:

1. It must be possible to use all the available data of activation, independently of their cross-section shapes,

2. The solution must approximate the  $A_i$  values in the best possible way, at the same time producing realistic spectral shapes (non-oscillating spectra, no negative-flux values).

Then, we can expand the flux as

$$\phi(E) = W(E) \sum_{k=1}^n a_k \psi_k(E) \quad (19)$$

The shape of the spectrum T1 used currently (see Table A.2) is described by the following function:

$$\phi(E) = (e^{-2.3E} + .03e^{-.75E}) e^{-\frac{1}{0.5+E}}$$

The best approximation to  $\phi(E)$  is assumed to be the one minimizing the quadratic form:

$$Q(t; a_1, \dots, a_t) = \sum_{i=1}^n \left( \frac{A_i - \int \sigma_i(E) \phi^t(E) dE}{A_i} \right)^2 \quad (20)$$

where  $t=1, 2, \dots, n$ .

$$\phi^t(E) = W(E) \sum_{k=1}^t a_k \psi_k(E)$$

if  $m$  = optimum value of the expansion terms,

$\phi^m(E)$  = related approximation,

$n$  = number of detectors.

then the only condition is  $m \leq n$ .

The requirement of minimum  $Q(t)$  is

$$\frac{\partial Q(t)}{\partial a_j} = -2 \left( \sum_{i=1}^n r_{ij} - \sum_{i=1}^n r_{ij} \sum_{k=1}^t a_k r_{ik} \right) = 0 \quad (21)$$

$j=1, \dots, t$

where  $r_{ij} = S_{ij}/A_i$ , and leads to the matrix form:

$$R^T R a = R^T e, \quad (22)$$

where:

$$a = \begin{pmatrix} a_1 \\ a_2 \\ \cdot \\ \cdot \\ \cdot \\ a_t \end{pmatrix} \quad e = \begin{pmatrix} 1 \\ 1 \\ \cdot \\ \cdot \\ \cdot \\ 1 \end{pmatrix} \quad R = \begin{pmatrix} r_{1,1} \cdots \cdots \cdots r_{1,t} \\ \cdot \\ \cdot \\ \cdot \\ \cdot \\ r_{t,1} \cdots \cdots \cdots r_{n,t} \end{pmatrix}$$

$R^T$  indicates the transpose of the matrix  $R$ .

Errors are caused by the following:

1. inaccuracy of the hypothesis expressed by Equation 19,
2. round-off errors in the numerical procedures,
3. experimental errors in the activation rates,
4. inaccuracy in the values of the cross-sections.

With regard to the last two points, the form of standard errors are

$$A_i \pm h_i A_i.$$

and

$$\sigma_i(E) \pm k_i \sigma_i(E)$$

where  $h_i$  and  $k_i$  will be suitably chosen then the evaluation of errors in the computed spectral shape is the form

$$\phi(E) \pm e(E)\phi(E)$$

where  $e(E)$  is the percent statistical error.

The numerical tests suggest the following:

1. The errors have an oscillating character that is related to the poles and zeros of the functions chosen for the series expansion.
2. The errors grow linearly with the errors in the input data.
3. The error grows when the number of detectors used is reduced.
4. The error grows when the number of terms in expansion increases, this fact may be related to the observations about the stability of the system.
5. The statistical error appears greatest in the regions where the solutions approximate the test spectrum in the worst way.

The role of the weighting function,  $W(E)$ , is important in the solution of the problem, because the expression of Equation 19 may be interpreted in the following sense: the unknown flux is obtained from the shapes of the function  $W(E)$  through the deformation described by the series expansion.

Comment 3 is important since, in order to obtain good results, it is necessary to use the maximum number of available detectors.

Comment 4 suggests a reduction in the number of

expansion terms used; but this may be in contrast with the choice suggested by the minimization of  $Q$ . For example, minimum value of  $Q$  may suggest the choice  $m=6$ , but with  $m=4, 5$  very similar; then the solution must be chosen between  $\phi^4, \phi^5, \phi^6$ .

If the input errors are 2.5%,  $\phi^5$  and  $\phi^6$  seem to be equivalent from the point of view of the reliability. But, if the input errors are increased to 5%,  $\phi^4$  is preferred, because its statistical errors are lower.

### C. SPECTRA CODE [5,6]

In the SPECTRA code, the flux is approximated by piecewise linear functions of energy and Equation 1 is reduced to the matrix form

$$A = C\phi \quad (23)$$

where  $A$  is an  $n \times 1$  vector whose entries are the measured activities,  $\phi$  is an  $m \times 1$  vector whose entries are the desired flux values, and  $C$  is an  $n \times m$  matrix whose elements are certain integrals of the cross-sections. The differential flux  $\phi(E)$  in the interval  $E_i$  to  $E_{i+1}$  is given by

$$\phi(E) = \phi_{i+1} \left( \frac{E - E_i}{E_{i+1} - E_i} \right) + \phi_i \left( \frac{E_{i+1} - E}{E_{i+1} - E_i} \right). \quad (24)$$

It is assumed that there is no differential flux below  $E_1$  and that the differential flux value at  $E_m$  is zero, that is,  $\phi_m = 0$ , and



$$\begin{aligned}
A_k &= \int_{E_1}^{E_2} \left[ \phi_2 \left( \frac{E - E_1}{E_2 - E_1} \right) + \phi_1 \left( \frac{E_2 - E}{E_2 - E_1} \right) \right] \sigma_k(E) dE \\
&+ \int_{E_2}^{E_3} \left[ \phi_3 \left( \frac{E - E_2}{E_3 - E_2} \right) + \phi_2 \left( \frac{E_3 - E}{E_3 - E_2} \right) \right] \sigma_k(E) dE \\
&+ \dots \\
&+ \int_{E_{m-1}}^{E_m} \left[ \phi_m \left( \frac{E - E_{m-1}}{E_m - E_{m-1}} \right) + \phi_{m-1} \left( \frac{E_m - E}{E_m - E_{m-1}} \right) \right] \sigma_k(E) dE \quad (25)
\end{aligned}$$

and the entries of  $C$  are given by

$$C_{ji} = \int_{E_{i-1}}^{E_i} \left( \frac{E - E_{i-1}}{E_i - E_{i-1}} \right) \sigma_j(E) dE + \int_{E_i}^{E_{i+1}} \left( \frac{E_{i+1} - E}{E_{i+1} - E_i} \right) \sigma_k(E) dE \quad (26)$$

In order to solve Equation 23, it is assumed that the first  $n \times n$  submatrix of  $C$  is nonsingular, where  $n$  is the rank of  $C$ . If the calculated activities are denoted by  $A_c$ , then the least squared difference,  $E$ , between the measured activity,  $A$ , and the calculated activity is given by  $E = (A_c - A)^T (A_c - A)$ . The function  $E$  is minimal with respect to  $\phi_c$  when

$$\frac{\partial E}{\partial \phi_c} = 0 \text{ and } \frac{\partial^2 E}{\partial \phi_c^2} \text{ is positive definite with } A_c = C\phi_c,$$

$\frac{\partial E}{\partial \phi_c} = 2(C^T C \phi_c - C^T A_c) = 0$ , and, if  $C^T C$  is nonsingular, the desired solution is  $\phi_c = (C^T C)^{-1} C^T A_c$ . When  $m > n$ , the matrix  $C^T C$  is singular and a unique solution in the least squared sense does not exist.

We defined a new error function as

$$E_1 = (A_c - A)^T (A_c - A) + (\phi - \phi_0)^T (\phi - \phi_0), \quad (27)$$

where  $\phi_0$  is an approximate solution. Differentiating the new error function with respect to  $\phi_1$  and equating to zero yields

$$\frac{\partial E_1}{\partial \phi} = 2C^T (A_c - A) + 2I^T (\phi - \phi_0) = 0 \quad (28)$$

and  $\frac{\partial^2 E_1}{\partial \phi^2} = C^T C + I$ . If  $\frac{\partial^2 E_1}{\partial \phi^2}$  is positive definite,

a unique solution of equation (28) exists which minimizes the error function. Since, if  $B$  is an  $m \times m$  positive (semi-)definite matrix and  $F$  is an  $m \times m$  diagonal matrix with non-negative entries, then  $B + F$  is positive definite, thus, the matrix  $C^T C + I$  is positive definite.

Suppose  $C^T (C\phi - A) = 0$ , the matrix  $C = (X, Y)$  where  $X$  is an  $n \times n$  nonsingular matrix and  $C^T = \begin{pmatrix} X^T \\ Y^T \end{pmatrix}$ . Now  $X^T$  has an inverse and  $\left[ (X^T)^{-1}, 0 \right] \begin{pmatrix} X^T \\ Y^T \end{pmatrix} [C\phi - A] = I (C\phi - A) = 0$ , which implies  $(C\phi - A) = 0$ , that is, the vector  $\phi$  is a solution to the equation  $C\phi = A$ . If we define the matrix

$$F = (C^T C + I)^{-1} \quad (29)$$

$$B = FC^T A \quad (30)$$

then we obtain an iterative algorithm,

$$\phi_{i+1} = B + F\phi_i. \quad (31)$$

Repeated applications of the algorithm yields the

matrix series

$$\phi_n = (I + F + \dots + F^{n-1}) B + F^n \phi_0, \quad (32)$$

since the matrix  $C^T C$  is positive definite which implies the eigenvalues of  $C^T C + I$  are greater than 1. Thus the eigenvalues of  $F$  are between zero and one, which implies  $F^n \rightarrow 0$  and  $I + F + F^2 + \dots$  converges to  $(I + F)^{-1}$ , thus obtaining the solution  $\phi = (I - F)^{-1} B$ . From the definition of  $F$ , we have  $F(C^T C + I) = I \rightarrow I - F = FC^T C \rightarrow \phi = (FC^T C)^{-1} B = (FC^T C)^{-1} FC^T A = I\phi$ , where  $\phi$  is the unique solution of  $C^{-1} A$ .

Since the error  $E_1$  is strictly monotonically decreasing if  $\phi_0$  is not a solution to  $A = C\phi$ , then we can use the iterative method to solve the Equation 23. Because  $\lim_{n \rightarrow \infty} E\phi_n = 0$ ;  $\lim_{n \rightarrow \infty} \phi_n$  exists and is a solution to  $A = C\phi$ .

The methods of SPECTRA are based on the above theory. Experience has led to several observations concerning the use of the proposed method. At first, it should be recognized that in the overdetermined condition, the solution values one obtains are somewhat dependent upon the trial solution. This characteristic is, of course, by choice since the method is designed to take advantage of any additional physical information one has about the spectral distribution. This physical information may be only qualitative; for example, the

spectrum might be thought to be a softened fission spectrum, a fusion spectrum; or one might have an actual crude theoretical spectrum which can be used. Secondly, errors in activation measurements, as in other techniques for solving this system of equations, can be magnified in the calculated flux. That is, a fractional error in one of the activities can cause a much larger error in one or more of the discrete differential flux values rather than distributing the error over the entire region of sensitivity. Thirdly, even without error in the activities, the calculated flux will sometimes show structure about the actual spectral shape due to the manner in which the initial trial function is perturbed by the detector response functions. This is particularly noticeable when it is necessary for the code to modify the trial flux considerably to obtain a solution.

## IV. RESULTS AND DISCUSSION

There are four sets of activities presented, three measured and one estimated. The first set contains 10 foils. These reactions are  $\text{In}115(n,n')\text{In}115m$ ,  $\text{Mg}24(n,p)\text{Na}24$ ,  $\text{Ni}58(n,p)\text{Co}58$ ,  $\text{Th}232(n,f)\text{FP}$ ,  $\text{U}235(n,f)\text{FP}$ ,  $\text{U}238(n,f)\text{FP}$ ,  $\text{Al}27(n,\text{He})\text{Na}24$ ,  $\text{Cu}63(n,G)\text{Cu}64$ ,  $\text{Fe}54(n,p)\text{Mn}54$ ,  $\text{Au}197(n,G)\text{Au}198$ . These are the test data of the SAND II code. The second set has 5 foils, that is,  $\text{Al}27(n,p)\text{Mg}27$ ,  $\text{Al}17(n,\text{He})\text{Na}24$ ,  $\text{Cu}63(n,G)\text{Cu}64$ ,  $\text{Fe}56(n,p)\text{Mn}56$ ,  $\text{Ni}58(n,p)\text{Co}58$ . These activities are obtained from UMR Reactor. The third and fourth sets contain the same 7 foils. These are  $\text{Al}27(n,\text{He})\text{Na}24$ ,  $\text{In}115(n,n')\text{In}115m$ ,  $\text{Al}27(n,p)\text{Mg}27$ ,  $\text{Fe}54(n,p)\text{Mn}54$ ,  $\text{Fe}56(n,p)\text{Mn}56$ ,  $\text{Mg}24(n,p)\text{Na}24$ ,  $\text{Ni}58(n,p)\text{Co}58$ . The former are from Henry A. Till [7]. Because all program codes got very poor results using these activity data, the fourth set is estimated values based on the results using the third set run in the SAND II code.

In order to fit these four sets of data, the first thing must be to obtain the input (or trial) spectrum. The differential neutron spectrum of the UMR Reactor at core position C3 (see Appendix F or Ref. 7) is used in second, third and fourth sets to fit all the three computer codes.

The highest energy value in the SAND II test data

is only 3 Mev, but it should be generated up to 18 Mev. One way to get this entire spectrum is from the first approximation spectrum in the SAND II code. It is easily seen that it is reliable because the errors between the input flux and the first approximation flux are all less than 5 percent.

The criteria of the comparison will be based on the computer time required, the calculated-to-measured activity ratio, the complexity of input data, and the obtained information from the output.

#### A. COMPUTER TIME REQUIRED

The RDMM code is the best one based on this criteria (see Table 1). Both SAND II and SPECTRA codes have free field input and iterative processes that use much time in data transmissions and iterations. The plot subroutine GRAF in the SAND II code uses nominally 120 minutes or \$36.- per case on the Calcomp Model 556 Digital Incremental Plotter. A major portion of this plotting time is occupied by the drawing of variable log-log grid.

#### B. CALCULATED-TO-MEASURED ACTIVITY RATIOS

There seems to be little difference between the three codes in this category. The RDMM code results in Table 2 are from the approximation order 6 of Monte Carlo histories. In the 5-foil case, the order of the

approximation polynomial,  $MAX=6$ , is greater than the number of foils,  $NS=5$ . In the case of 10 foils, the reason for these ratios of foils  $Au197(n,G)Au198$  and  $Cu63(n,G)Cu64$  poor results in the RDMM and SPECTRA codes is the former foil activity sensitivity range being from  $4.75 \times 10^{-6}$  to  $3.4 \times 10^{-2}$  Mev and the latter foil activity sensitivity range being from  $5.75 \times 10^{-4}$  to .12 Mev. Perhaps, these two codes do not have enough information on cross-sections in this range. These are gamma reactions, and the cross-section for the gamma reaction is generally very low in the fast neutron range.

In the third case with 7 foils, the RDMM code had one negative ratio for the  $Al27(n,p)Mg27$  reaction, and the SPECTRA code had one for the  $In115(n,n')In115m$  reaction. From Equation 1, recall that the calculated activation rate is defined as the summation of the product of neutron cross-section and neutron differential flux. We use the  $Al27(n,p)Mg27$  reaction to illustrate the reason why these ratios sometimes were negative. Because the RDMM code gave high negative flux within a wide energy range from 3.1 to 7.9 Mev (see Figures 5 and Appendix C), then, the calculated activation rate became a negative value.

The relationships of activation rates between the codes should be used carefully (see Appendix B). Some recommendations in using data are listed in Appendix D.

### C. COMPLEXITY OF INPUT DATA

It seems to be that the SPECTRA code is the best one based on this criteria (see Appendix A). The RDMM code requires hundreds of cards for cross-section information in each case. If someone were to run two cases with the same foils in each, then he should duplicate these data decks. However, it seems to be inefficient and ambagious work.

The SAND II code is only slightly more complicated than the SPECTRA code. One thing has to be noticed in the SAND II and SPECTRA codes is that the foil name used must be the same as the foil name in the library file (see Appendix C). One should notice the relations among the codes.

### D. OUTPUT

There are detailed descriptions for the output forms of each code in Appendix E.

In order to compare the three codes, four sets of data were run in each computer code. These results were then plotted by the Calcomp Model 556 Digital Incremental Plotter in the same unity. (see Figures 1 to 8)

The reasons for any discontinuity in the flux curve are: the flux is extremely low, or the flux has a negative value. The first happened nine to ten in the SAND II code. The second always happened in the RDMM and SPECTRA



codes, but, never occurred in the SAND II code. The SAND II code never yielded a negative flux values.

From Figures 1 and 2, the SPECTRA code appears to be the worst one, but it still agrees at the high energy range, say above 9 Mev, after the use of subroutine REPETE. In the Figures 3 and 4, the RDMM results are nearly perfect except there is not indicated peak at 14-15 Mev. The results of subroutine LIMIT in the SPECTRA code seems to be better than the RDMM code above 7 Mev. It is interesting to note, if we connect two discontinuous points in the curve of LIMIT these seems to be a good fit of the trial flux. The differential flux obtained from the SAND II code has an obvious peak at 6 Mev, but this peak does not occur in Figures 5 or 7 (both were calculated with the same trial flux), so that this peak is not real. From Figure 5, it seems that no code could fit the trial flux due to the large standard deviation of activation rate. But the RDMM and SPECTRA codes seem good in the high energy range, say above 9 Mev.

In Figures 7 and 8, the results from subroutine LIMIT and REPETE of SPECTRA code are very reasonable, especially, at the high energy range. And if we use three or more points smoothing method, we could get a good result.

With reference to the differential flux or the

integral flux, the RDMM and SPECTRA codes seem better than the SAND II code. All in all, it could be said that the SPECTRA code is better than the other two for the UMR Reactor neutron spectrum.

Table 1  
Computer Time Required Comparison

		SAND II		RDMM		SPECTRA	
		Time	Cost	Time	Cost	Time	Cost
Linkedit (average)		24.11	\$0.84	10.37	\$0.36	19.80	\$0.69
GO	Minimum	3:30.00	\$7.35	1:40.00	\$3.50	7:20.00	\$15.40
	Normal	5:30.00	\$11.55	1:50.00	\$3.90	12:00.00	\$25.20
PLOT		120:00.00	\$36.00				
Total		6:00.00	\$48.40	2:00.00	\$4.20	12:20.00	\$25.90

Table 2  
Calculated-to-Measured Activity Ratios

Test	Reaction	SAND II	RDMM	SPECTRA
10 Foils	Al27(n,He)Na24	1.06997	0.97485	0.99999
	Au197(n,G)Au198	1.00090	0.29267	0.50101
	Cu63(n,G)Cu64	1.00180	0.62646	1.20329
	Fe54(n,p)Mn54	0.92894	0.76501	1.00049
	In115(n,n')In115m	1.09027	1.22863	0.99801
	Mg24(n,p)Na24	0.94313	1.04523	0.99998
	Ni58(n,p)Co58	0.91550	1.25435	0.99955
	Th232(n,f)FP	1.09230	0.77167	0.99842
	U235(n,f)FP	1.00311	1.24901	1.00674
	U238(n,f)FP	1.00160	0.83642	1.00203
5 Foils	Al27(n,He)Na24	1.57704	1.00000	0.99982
	Al27(n,p)Mg27	1.92790	1.00000	0.99938
	Cu63(n,G)Cu64	1.13186	1.00000	0.81726

Table 2 (continue)  
Calculated-to-Measured Activity Ratios

Test	Reaction	SAND II	RDMM	SPECTRA
5 Foils (continue)	Fe56(n,p)Mn56	0.48237	1.00000	1.00324
	Ni58(n,p)Co58	1.12271	1.00000	1.00112
7 Foils Version III	Al27(n,He)Na24	0.95193	1.00104	0.99648
	Al27(n,p)Mg27	1.01184	1.00231	1.00268
	Fe54(n,p)Mn54	1.04833	0.99092	1.00435
	Fe56(n,p)Mn56	0.97286	0.99678	0.99354
	In115(n,n')In115m	1.02020	1.00009	0.99989
	Mg24(n,p)Na24	0.95548	1.00067	1.00587
	Ni58(n,p)Co58	1.04976	1.00000	0.99472
7 Foils No Version	Al27(n,He)Na24	10.86956	0.55022	0.00288
	Al27(n,p)Mg27	0.23375	-0.00533	0.00066
	Fe54(n,p)Mn54	833.33333	0.99964	1.02572

Table 2 (continue)

## Calculated-to-Measured Activity Ratios

Test	Reaction	SAND II	RDMM	SPECTRA
7 Foils No Version (continue)	Fe56(n,p)Mn56	0.57399	0.02445	0.00017
	In115(n,n')In115m	1.29049	0.87005	-0.00796
	Mg24(n,p)Na24	22.37136	1.23879	0.00395
	Ni58(n,p)Co58	14.94768	1.01434	0.09084

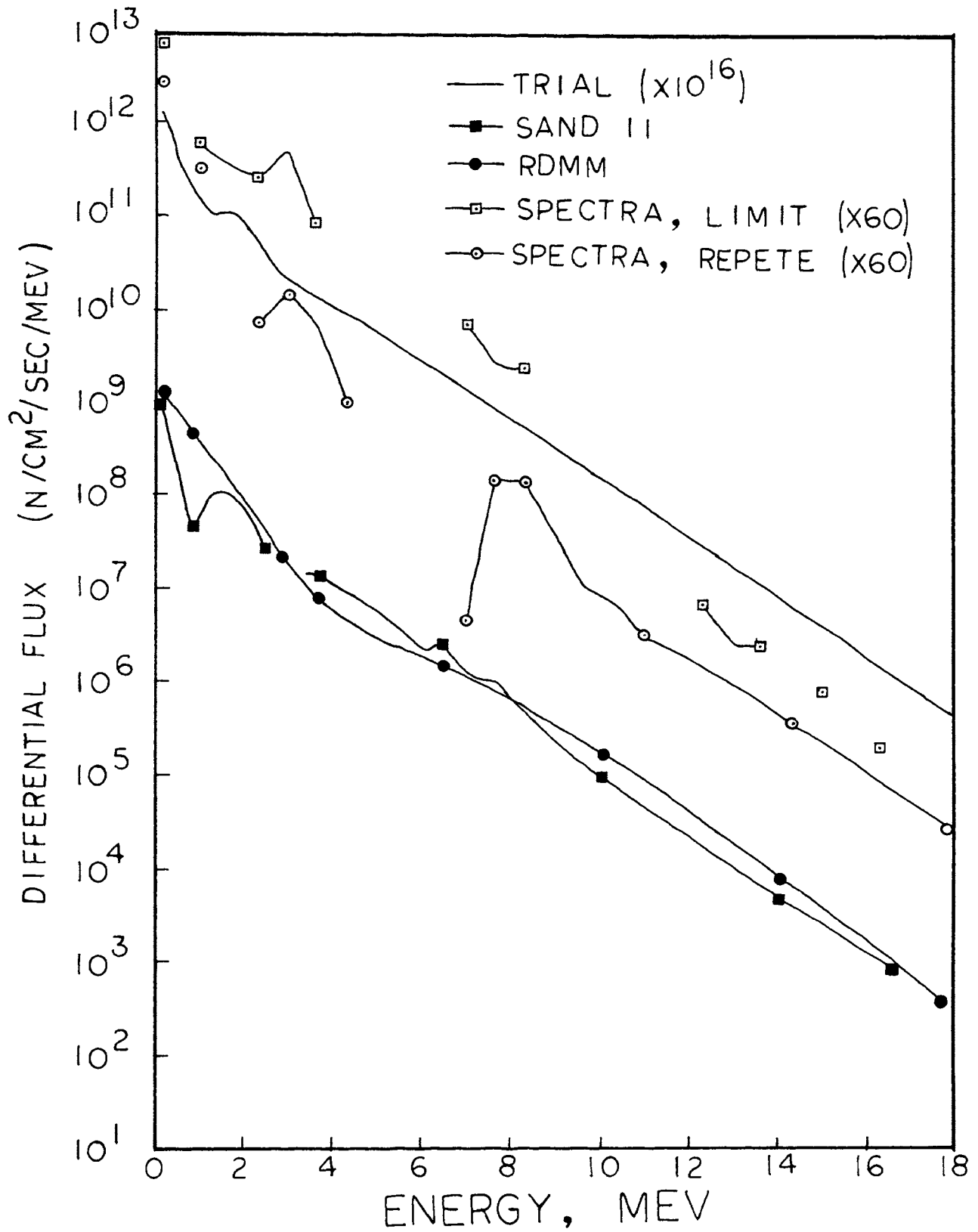


Figure 1. Neutron differential spectrum for 10 foils.

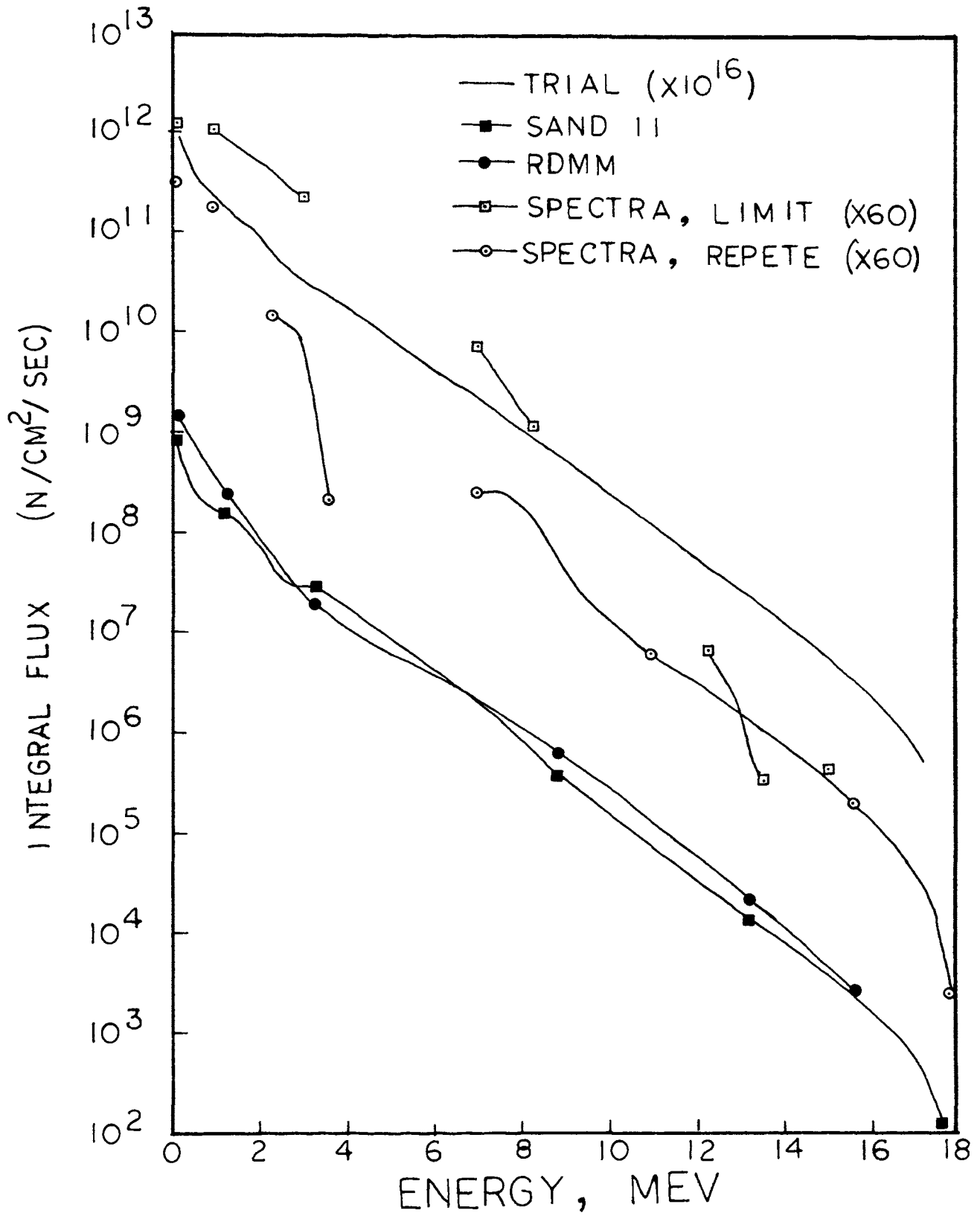


Figure 2. Neutron integral spectrum for 10 foils.



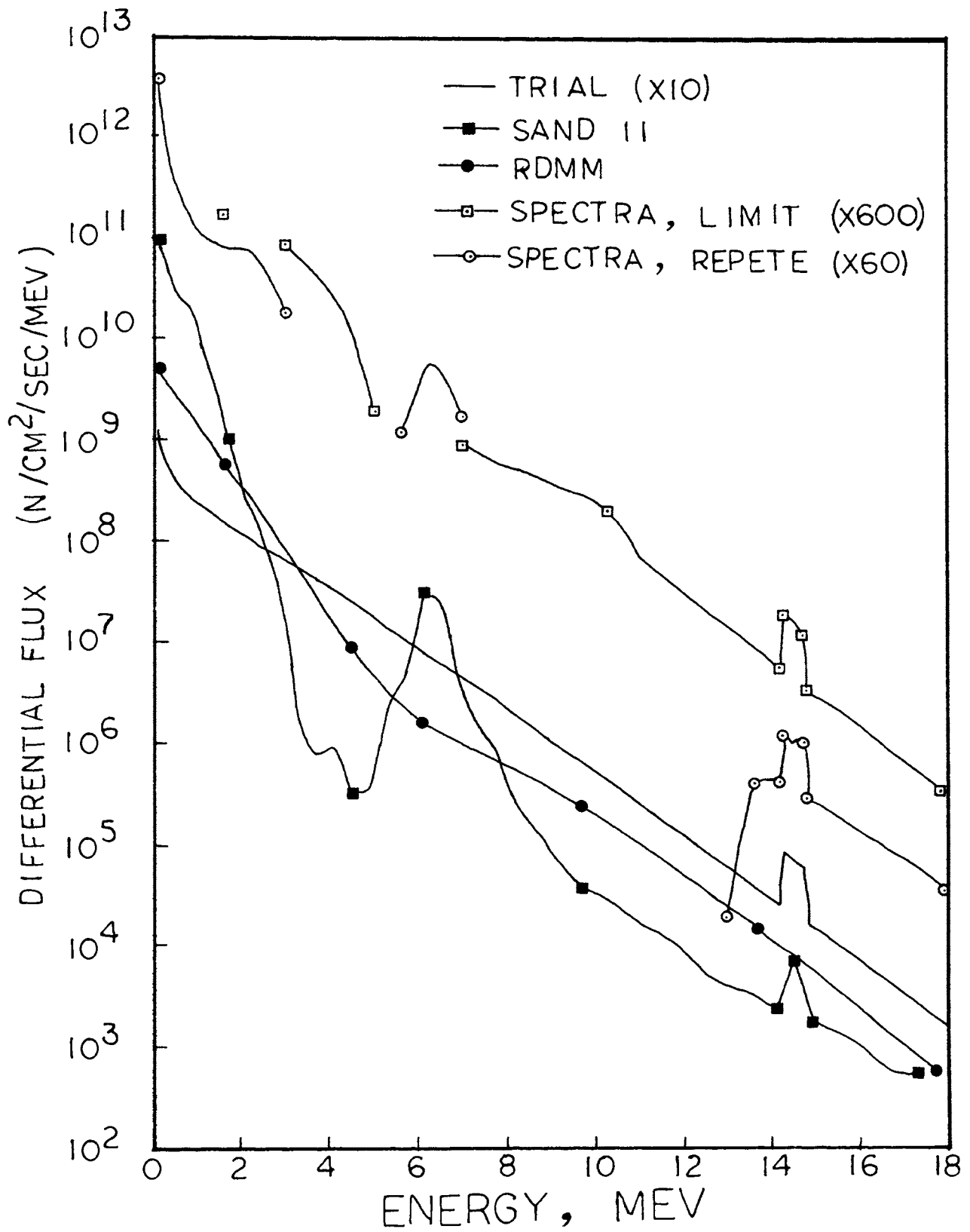


Figure 3. Neutron differential spectrum for 5 foils.

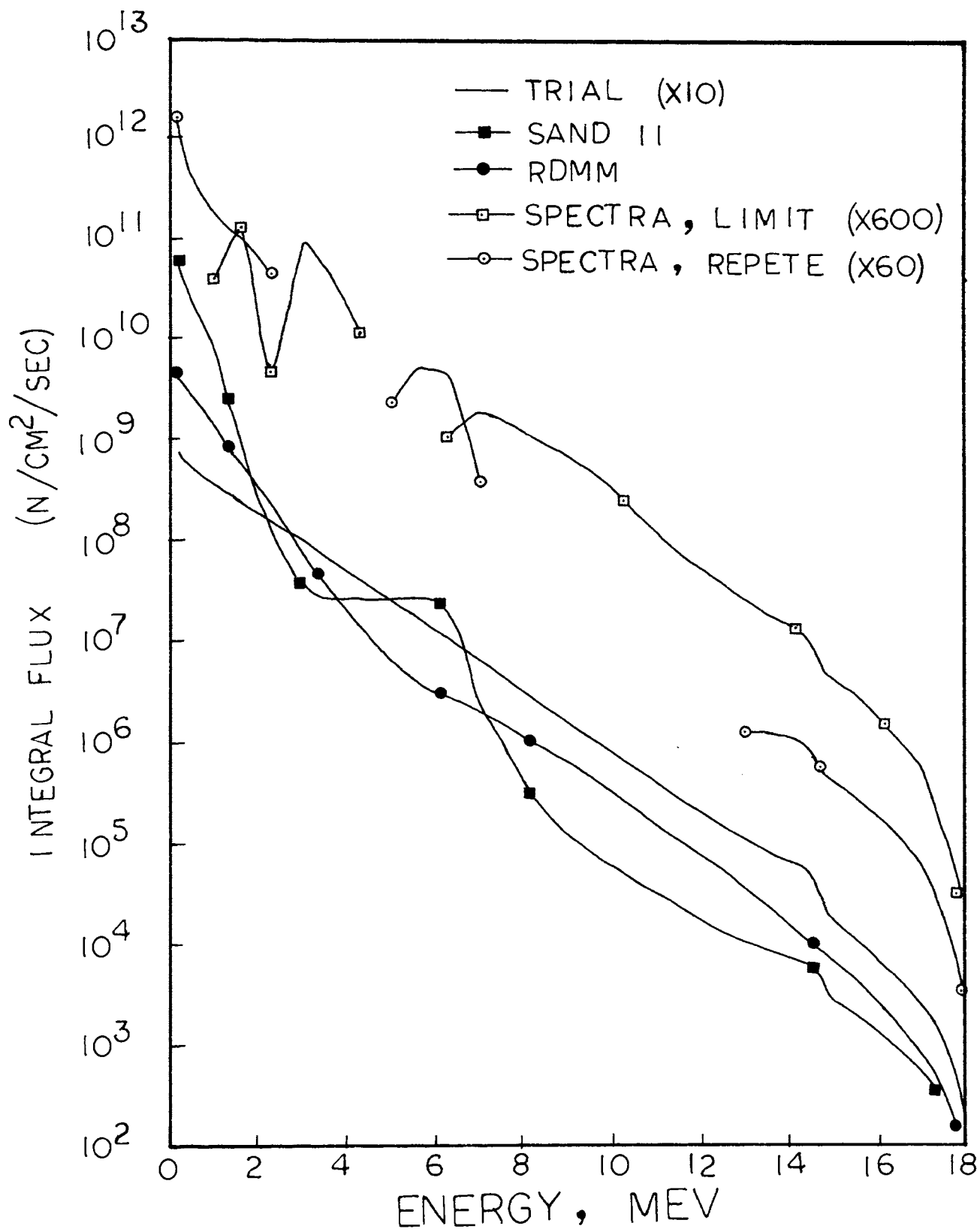


Figure 4. Neutron integral spectrum for 5 foils.

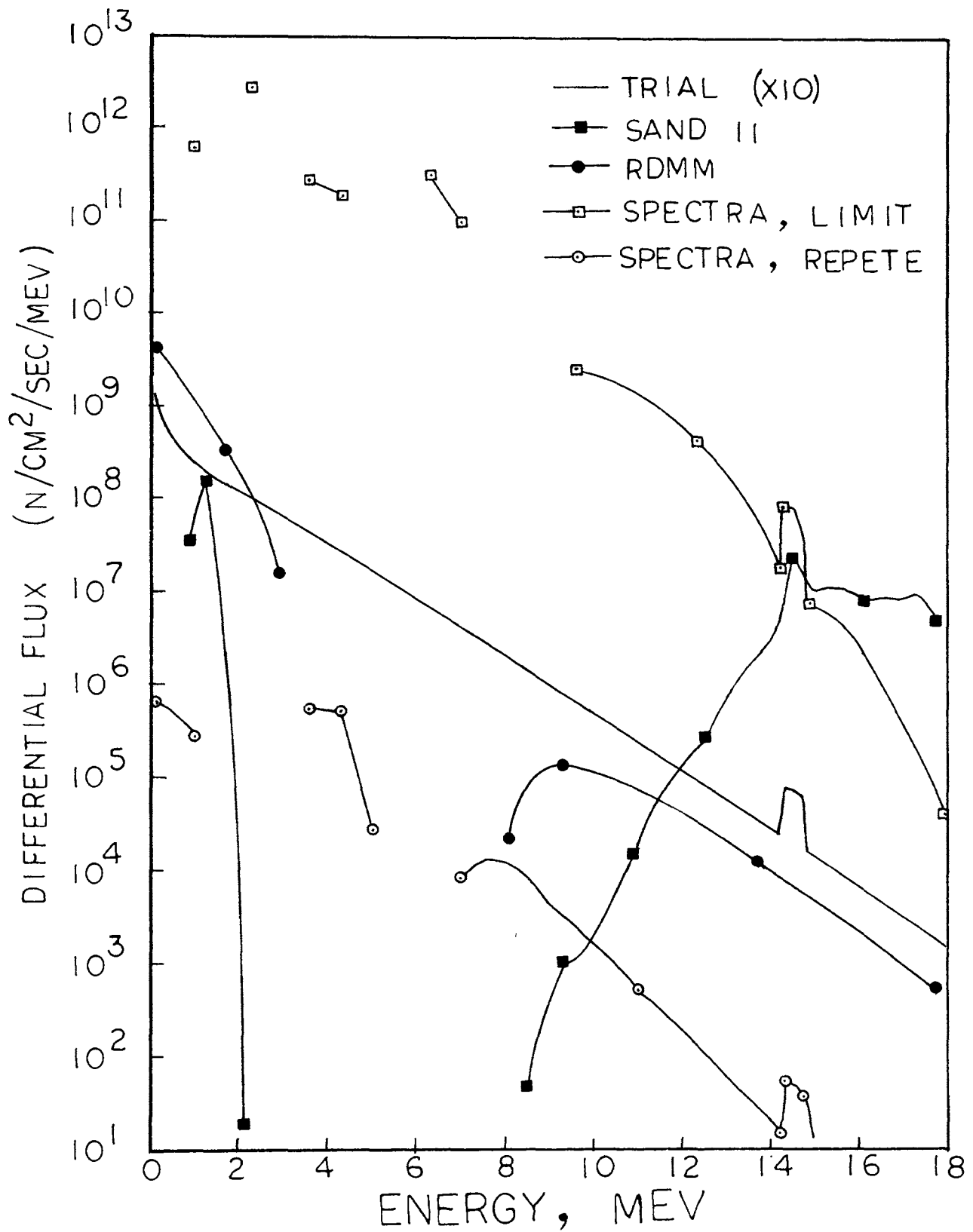


Figure 5. Neutron differential spectrum for 7 foils, no version.

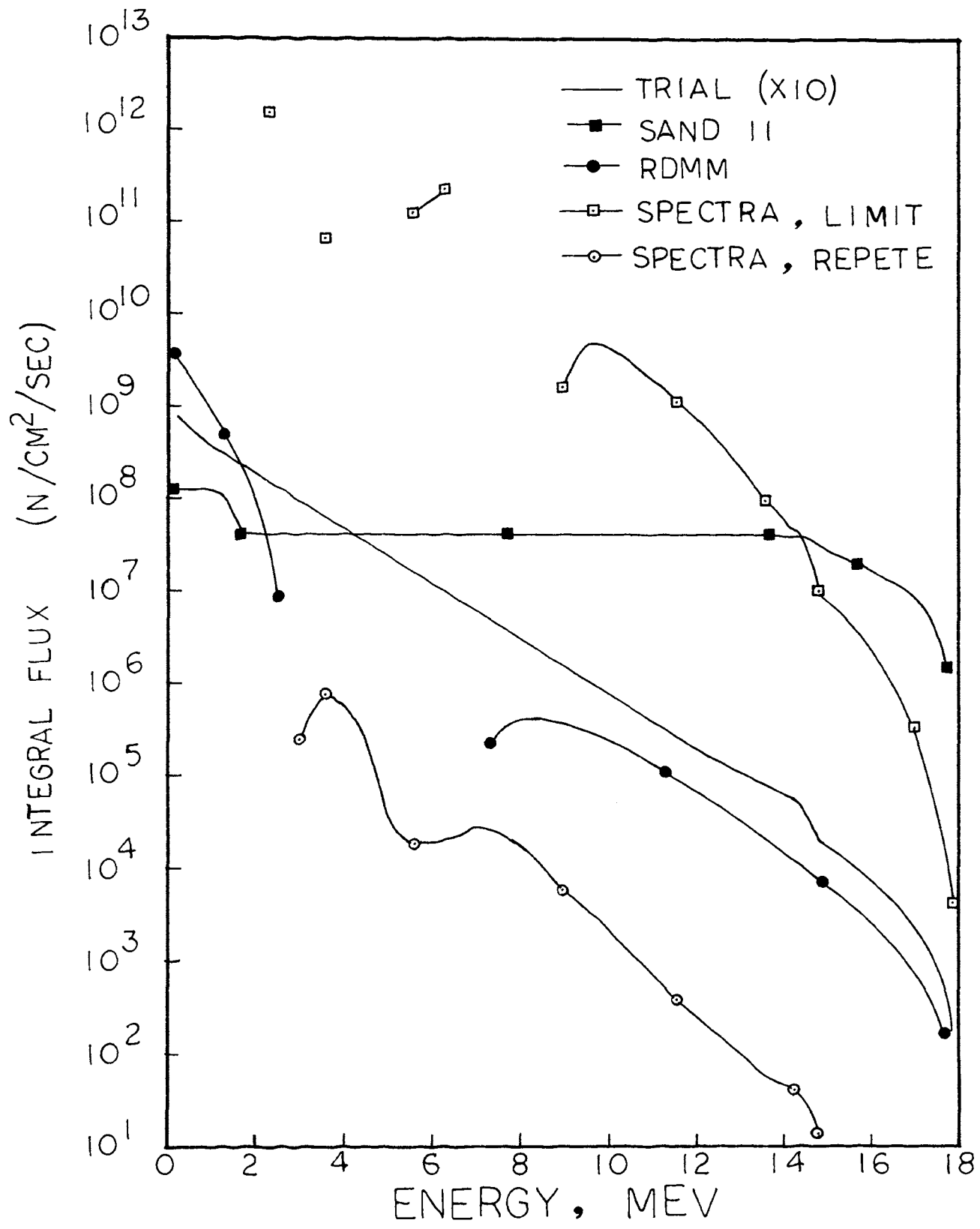


Figure 6. Neutron integral spectrum for 7 foils, no version.

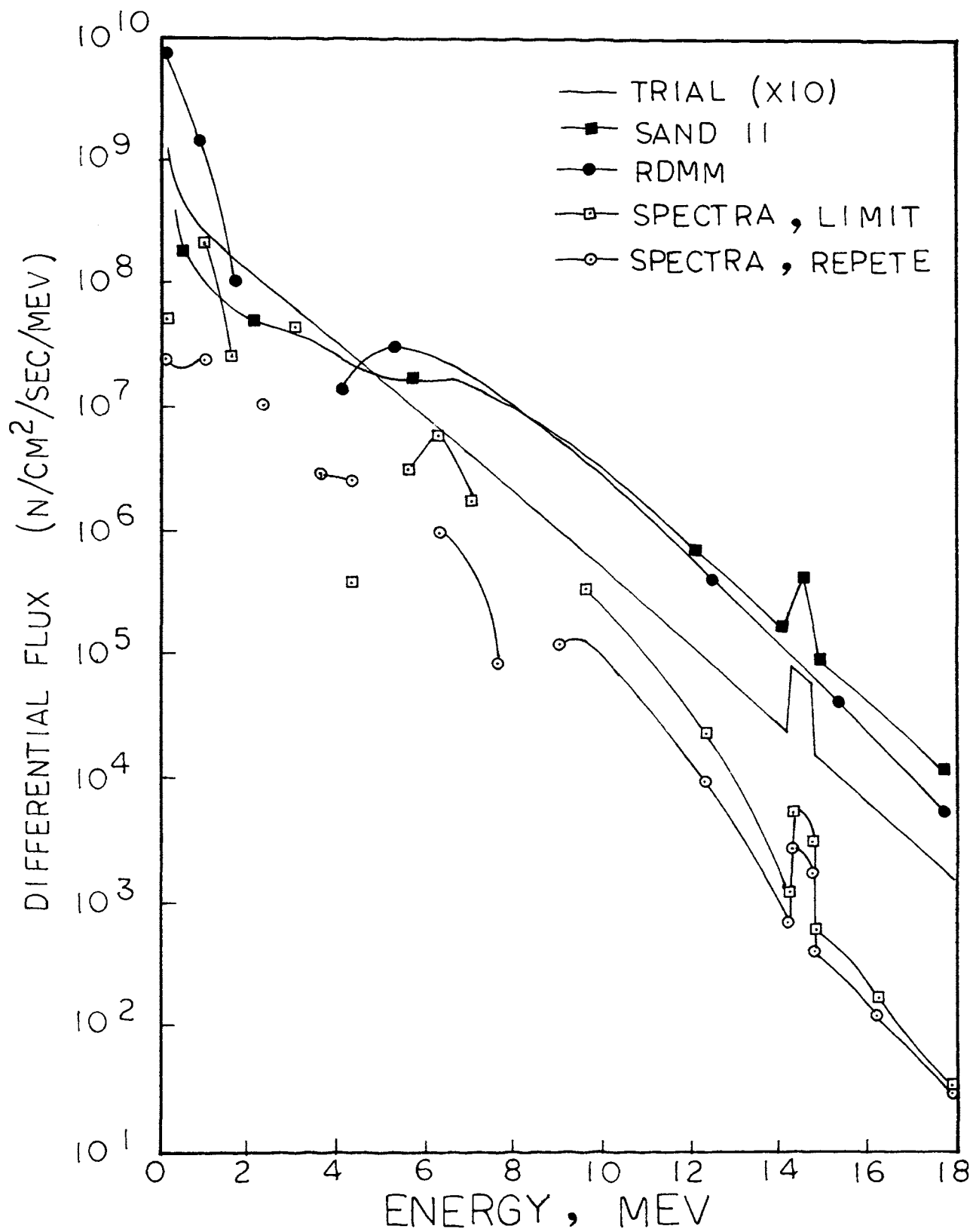


Figure 7. Neutron differential spectrum for 7 foils, version III.

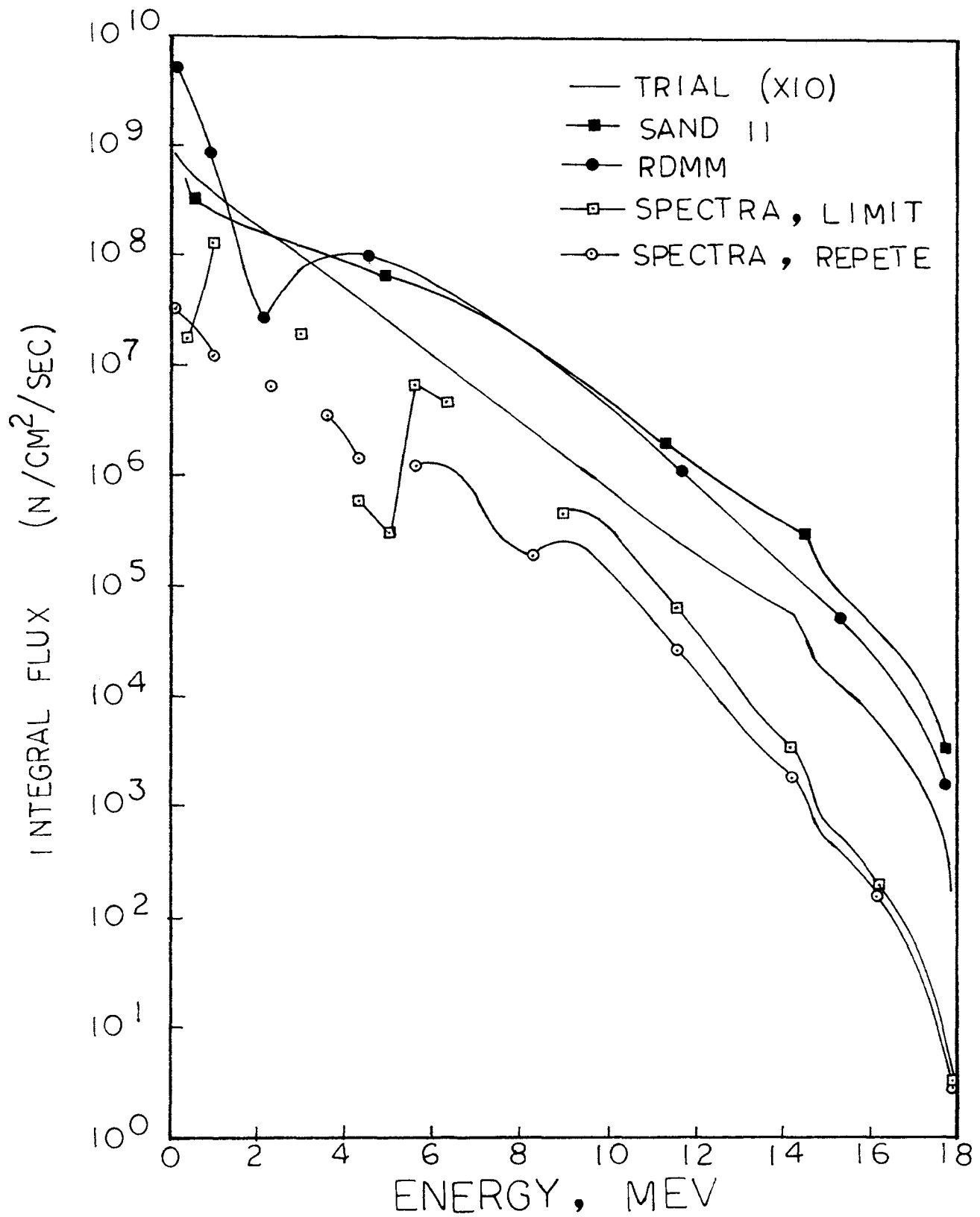


Figure 8. Neutron integral spectrum for 7 foils, version III.

## V. CONCLUSIONS

In the preceding section, we have compared the three codes from four viewpoints, that is, computer time required, the calculated-to-measured activity ratios, complexity of input data, and information obtained from the output.

Considering the computer time saving, the RDMM code appears to be the optimal code. The RDMM code yields satisfactory results, especially at the high values. We could extrapolate the curve from high energy to low energy. But, it does not follow any peaks in the trial flux. Perhaps, this is not serious in the case of narrow peak widths.

For satisfying the criteria of the simplest data input, the best output results, and the activity ratios, the SPECTRA code appears to be the best one among these three computer codes. Although the SPECTRA code takes much computer time, it still costs less than the SAND II code if the latter is run under a plotting situation.

## VI. RECOMMENDATIONS

The scope of the present codes did not permit all the effort which is known to be required to optimize the computer codes. Several areas of effort are recommended below which will either increase the codes' utility or correct current weaknesses. No indication of priority is intended in the order of discussion.

### A. SAND II CODE

The program should be modified to monitor each iteration. Currently, if the time specified by the user in the limit card is exceeded, execution terminates with no further output, essentially wasting the entire run. The provision should be included to initiate step printout of running results (specially, at the fast neutron region) such as in the RDMM code.

A study should be initiated to accelerate toward the solution using some well-known successive iterative process such as, say, Aiken's  $\delta^2$  procedure [9]:

$$\phi_j^{(0)'} = \frac{\phi_j^{(k+1)}\phi_j^{(k-1)} - (\phi_j^{(k)})^2}{\phi_j^{(k+1)} + \phi_j^{(k-1)} - 2\phi_j^{(k)}}, \quad j=1, \dots, m$$

This may result in significant savings in execution time.

It should be reprogrammed in the plot subroutine GRAF to plot the marginal line with log incremental grid indicated by tic marks in place of the complete log-log plots. This should reduce the plotting time



from nominally 120 minutes to 20 minutes.

#### B. RDMM CODE

The available program should be written to read the foil cross-section information from a tape. This procedure would involve substantial reprogramming of the code, but it would result in effectively simplifying the data input.

The subroutine PESI should be suitably changed in accordance with the shape of neutron spectrum used. This may result in significant spectrum responses.

#### C. SPECTRA CODE

The iteration process should be modified to save executive time in subroutine REPETE.

## APPENDIX A

## DATA FORMAT USED IN COMPUTER CODES

## A.1 SAND II CODE

All input data cards are read by SAND II code using subroutine VIF (except the first user's name card) and are therefore free from location and spacing format.

The following abbreviations and symbols are used:

- [ ] select one;
- ( ) omit if not need or desired;
- n integer number
- x "real" or "floating point" number;
- a alphameric character.

section -1: user's name, one card. Format: 5A4.

section 0: number of cases, one card.

n CASES

This card is to included only once, at the beginning of the entire data deck for a run.

section 1: title cards, as many cards as desired.

Taaa.....aaa.....  
" " " "

section 2: type of run, and type of activity measurement, one card.

[ ITERATION ] (TIME INTEGRATED)  
[ ACTIVITY ]

section 3: one card sepcifying number of foils, plus

one card for each foil.

n FOILS  
aaaaaaa (CADMIUM x) (BORON x) (GOLD x)  
 " " " "

section 4: for ITERATION RUN only: measured activities,  
 as many cards as needed.

ACTS x x x x ....  
 " " " " "

section 5: spectrum form, one card.

SPECTRUM [ LIBRARY (n)  
 FUNCTION n  
 TABULAR ]

section 6: for TABULAR SPECTRUM INPUT only: spectrum  
 tabulation, as many cards as needed.

n POINTS  
 ENER x x x x ....  
 " " " " "  
 " " " " "  
 FLUX x x x x ....  
 " " " " "  
 " " " " "

section 7: for ITERATION RUN only: solution parameters,  
 three cards.

LIMIT n  
 DEVIATION x  
 DISCARD x

section 8: extrapolation forms and normalization energy,  
 three cards.

LOW END [ E  
 SQ RTE  
 THERMAL (x) ]  
 HIGH END [ FISSION  
 FUSION ]

NORM x

section 9: auxiliary output, one card.

(NO) (PLOT) (NO) (CARDS)

section 10: for ITERATION RUN only: structure  
retardation, one card.

SMOOTH n

## A.2 RDMM CODE

RDMM is the only code to use format for the input data.

section 0: number of case, one card. Format: 10I6

section 1: title cards, two cards. Format: (9A8)

section 2: NS, NP, NPP card. Format: 10I6

NS = number of detectors, n

NP = number of points in which the  $\sigma(E)$   
are tabulated

NPP = step of the print-out results

section 3: MIN, MAX card. Format: 10I6

Minimum and maximum order for approximated  
polynomial.  $MAX \leq n$ .

section 4: number of Monte Carlo histories for each  
approximation order. Format: 10I6

section 5: E(1), H card. Format: 3E10.6

E(1) = the first energy value in which the  
 $\sigma_i(E)$  are tabulated (MeV).

H = step of the energy tabulation (MeV).

section 6: SIGNME(I). Format: 9A8. One card for the name of foil;

SIGMA(J). Format: 40X,F10.3/(5F10.3)  
cross-section of the foil I expressed in milli-barn for J=1,NP

section 7: activities and relative standard error on the A and SIGMA.

Format: 3E10.6

section 8: coef. of polynomial formula. Format: 8F10.0

section 9: auxiliary card, scale factor SCALE, and initial random digit IX. Format: E15.3,I8

### A.3 SPECTRA CODE

SPECTRA code is a "free field" input program (i.e., data fields are not determined by specified columns of a data card. For SPECTRA code, data should be punched in columns 1-72 and data fields are split by commas.

The following is the RUN Mode:

section 0: mode card, one card

RUN

This card is at the beginning for each case.

section 00: title cards, two cards

section 1: contains 5 fields, IFOIL, IENER, MODE, ERRE and MITE, in one card.

IFOIL = number of foils;

IENER = the total number of flux values including both endpoints;

MODE = 0 LIMIT only,  
1 REPETE only,  
2 both LIMIT and REPETE,  
3. ACTIVITY RUN;

ERRE = the required tolerance;

MITE = limit number for iteration.

section 2: contains 2\*IENER fields in increasing order of energy with the form energy value, flux value, energy value, flux value, etc.

section 3: contains 3 fields, ITYPE, AC, BI. One card for one foil.

ITYPE = name of the foil;

AC = activation rate;

BI = weight factor.

Table A.1 shows the 5 foils set of data used in SAND II code, Table A.2, A.3, in RDMM and SPECTRA code, respectively.

Table A.1. SAND II Code 5 Foils Data Set

CHEN JAU WEN

1 CASES

T TEST TO USE UMR REACTOR NEUTRON FLUX SPECTRUM AT CORE PSSITION C-3

T 5 FOILS, 1 POINT SMOOTHING

T

ITERATION

5 FOILS

NI58P CADMIUM 0.0508

CU63G CADMIUM 0.0508

FE56P CADMIUM 0.0508

AL27P CADMIUM 0.0508

AL27A CADMIUM 0.0508

ACTS 3.810-17 6.427-16 9.978-19 6.097-19 9.042-20

SPECTRUM TABULAR

91 POINTS

ENER	.1	.2	.4	.6	.8	1	1.2	1.4	1.6	1.8	2	2.2	2.4	2.6	2.8	3	3.2	3.4	3.6	3.8	4
ENER	4.2	4.4	4.6	4.8	5	5.2	5.4	5.6	5.8	6	6.2	6.4	6.6	6.8	7	7.2	7.4	7.6	7.8		
ENER	8	8.2	8.4	8.6	8.8	9	9.2	9.4	9.6	9.8	10	10.2	10.4	10.6	10.8	11	11.2	11.4			
ENER	11.6	11.8	12	12.2	12.4	12.6	12.8	13	13.2	13.4	13.6	13.8	14	14.2	14.4	14.6					
ENER	14.8	15	15.2	15.4	15.6	15.8	16	16.2	16.4	16.6	16.8	17	17.2	17.4	17.6						
ENER	17.8	18																			
FLUX	1.35+8	8.13+7	4.92+7	3.66+7	2.94+7	2.45+7	2.09+7	1.80+7	1.56+7	1.36+7											
FLUX	1.19+7	1.04+7	9.16+6	8.04+6	7.05+6	6.19+6	5.43+6	4.77+6	4.18+6	3.66+6											
FLUX	3.21+6	2.81+6	2.46+6	2.15+6	1.88+6	1.64+6	1.44+6	1.26+6	1.10+6	9.56+5											
FLUX	8.34+5	7.27+5	6.34+5	5.52+5	4.81+5	4.19+5	3.64+5	3.17+5	2.76+5	2.4+5											
FLUX	2.09+5	1.81+5	1.57+5	1.37+5	1.19+5	1.03+5	8.95+4	7.77+4	6.74+4	5.85+4											
FLUX	5.07+4	4.4+4	3.81+4	3.3+4	2.86+4	2.48+4	2.15+4	1.86+4	1.61+4	1.4+4											
FLUX	1.21+4	1.05+4	9060.	7840.	6780.	5870.	5070.	4390.	3800.	3290.	2840.										
FLUX	2450.	7600.	6570.	1580.	1370.	1180.	1020.	883.	763.	659.	569.	491.									
FLUX	424.	366.	316.	273.	236.	203.	175.	151.													

Table A.1. SAND II Code 5 Foils Data Set (continue)

LIMIT 25  
DEVIATION 5  
DISCARD 100.0  
LOW END E  
HIGH END FISSION  
NORM 1.0-10  
NO PLOT, NO CARDS  
SMOOTH 1



Table A.2. RDMM Code 5 Foils Data Set

1 CASES  
 I AM TESTING THIS CODE WITH THE SPECTRUM T1 BY UMRR SPECTRUM  
 RUN FOR ALTERNATE DECK USING 5 DETECTORS FOR SPECTRUM T1

5	180	4		
3	5			
100	100	100	100	
0.10 +00	0.10 +00			
NI58P				0.0
0.0	0.0	0.0	0.0	0.0
0.0	0.0	0.0	0.0	1.336
3.582	5.117	5.430	9.233	11.682
16.437	22.686	29.285	38.721	49.321
62.832	77.349	91.778	104.830	117.407
129.792	145.997	172.496	207.494	232.998
234.002	227.001	227.000	226.501	231.997
257.493	297.491	337.493	364.996	383.746
401.246	419.246	437.746	455.246	471.746
486.997	500.996	513.498	524.497	536.247
548.747	559.747	569.248	578.498	587.497
595.873	603.623	610.623	616.873	621.875
625.624	629.374	633.124	635.750	637.250
638.500	639.500	640.250	640.750	641.375
642.125	642.875	643.625	644.000	644.001
644.001	644.001	644.250	644.750	644.750
644.251	643.001	641.002	639.501	638.501
637.251	635.752	634.500	633.501	632.251
630.751	629.001	627.002	625.002	623.002
620.877	618.627	616.377	614.127	612.002
610.002	607.752	605.252	602.752	600.252
597.977	595.927	593.677	591.227	588.253

Table A.2. RDMM Code 5 Foils Data Set (continue)

584.753	581.753	579.253	577.002	575.002
572.004	568.004	564.503	561.503	558.253
554.753	551.378	548.128	544.628	540.879
536.504	531.505	526.754	522.254	516.506
509.506	503.005	497.006	490.257	482.757
475.257	467.757	460.506	453.507	444.760
434.260	423.760	413.260	401.013	387.013
371.266	353.766	335.019	319.511	309.634
300.884	292.133	283.383	274.633	265.883
257.133	248.383	239.633	230.883	222.084
213.235	204.386	195.537	186.688	177.839
168.989	160.140	151.291	142.442	133.518
124.519	115.520	106.521	97.522	88.522
79.523	70.524	61.525	52.526	

CU63G

\*\*\* 37 cards for cross-section \*\*\*

FE56P

\*\*\* 37 cards for cross-section \*\*\*

AL27P

\*\*\* 37 cards for cross-section \*\*\*

AL27A

\*\*\* 37 cards for cross-section \*\*\*

Table A.2. RDMM Code 5 Foils Data Set (continue)

3.8099E2	.05	.05					NI58P
6.4270E3	.05	.05					CU63G
9.9781	.05	.05					FE56P
6.0971	.05	.05					AL27P
.90422	.05	.05					AL27A
	1						
	1	-1					
	2	-4	1				
	6	-18	9	-1			
	24	-96	72	-16		1	
1.000E+19		5					

Table A.3. SPECTRA Code 5 Foils Data Set

```

RUN
UMR REACTOR FAST NEUTRON SPECTRUM AT CORE POSITION C-3
5 FOILS, 33 POINTS, LIMIT AND REPETE RUN 2,000 ITERATIONS
5, 33, 2, 1.0E-3, 2000
.01, .0, .1, 2.25E6, .4, 8.2E5, 1., 4.08E5, 1.6, 2.6E5, 2.3, 1.63E5,
3., 1.03E5, 3.6, 6.97E4, 4.3, 4.38E4, 5., 2.73E4, 5.6, 1.83E4, 6.3,
1.13E4, 7., 6983., 7.6, 4600., 8.3, 2817., 9., 1717., 9.6, 1123.,
10.3, 681., 11., 413., 11.6, 268., 12.3, 162., 13., 97.8, 13.6, 63.3,
14.2, 40.8, 14.3, 136., 14.5, 118., 14.7, 102., 14.8, 26.3, 15.5,
15.8, 16.2, 9.48, 17., 5.02, 17.2, 2.7, 18., .0
AL27(NHE)NA24 , 93.247 , .2
AL27(NP)MG27 , 59565.2 , .2
CU63(NG)CU64C40 , 330428. , .2
FE56(NP)MN56 , 2885.71 , .2
NI58(NP)CO58 , 164.328 , .2
ENDEND

```

## APPENDIX B

## RELATIONS FOR ACTIVITIES IN COMPUTER CODES

The most important information in each of the computer codes used are the activation rates.

The unit of activity in the SAND II code is dis/sec-nucleus. But, for numerical reasons, the order of magnitude must be in the range  $10^{-3}$  to  $10^3$  in the RDMM code. If the cross-sections are given in millibarns, then a scale factor of  $10^{19}$  is usually used for the activities as in the SAND II data. Therefore, a scale factor of  $10^8$  must be applied to the results in order to obtain differential flux values in the usual unit, n/cm<sup>2</sup>-sec-Mev, and integral flux values in n/cm<sup>2</sup>-sec.

In the SPECTRA code, the activity per unit mass (dis/min-gm) is used. If the cross-section  $\sigma_k$  data is in barns, then the activity in the SPECTRA code is scaled by  $60 \cdot N_0 \lambda / A$  as in the SAND II code, where  $N_0$  is the Avogadro's number,  $\lambda$  is the decay constant in min<sup>-1</sup>, and A is the atomic weight.

## APPENDIX C

## CROSS-SECTION INFORMATION USED IN COMPUTER CODES

SAND II and SPECTRA each contain a library of threshold cross-sections for 34 and 29 foil reactions, respectively.

The short reaction names in the SAND II library cross-section file named CSTAPE are as follows:

- |            |            |
|------------|------------|
| 1. NI58P   | 2. PU239F  |
| 3. SC45G   | 4. NA23G   |
| 5. TH232G  | 6. U238G   |
| 7. AU197G  | 8. CO59G   |
| 9. IN115G  | 10. MN55G  |
| 11. CU63G  | 12. U238F  |
| 13. TH232F | 14. ZN64P  |
| 15. FE54P  | 16. S32P   |
| 17. SI28P  | 18. S34A   |
| 19. MG24P  | 20. CL35A  |
| 21. NI582  | 22. I1272  |
| 23. ZR902  | 24. TI46P  |
| 25. TI47P  | 26. TI48P  |
| 27. CU632  | 28. P31P   |
| 29. FE56P  | 30. AL27P  |
| 31. NP237F | 32. U235F  |
| 33. AL27A  | 34. IN115N |

The reaction names in the SPECTRA library cross-section file named SPELIB are as follows:

- |                      |                      |
|----------------------|----------------------|
| 1. AL27(N HE)NA24    | 2. AL27(N P)MG27     |
| 3. AU197(N G)AU198C  | 4. CL35(N HE)P32     |
| 5. CO59(N G)CO60C40  | 6. CU63(N 2N)CU62    |
| 7. CU63(N G)CU64C40  | 8. FE54(N P)MN54     |
| 9. FE56(N P)MN56     | 10. I127(N 2N)I126   |
| 11. IN115(N N)115M   | 12. MG24(N P)NA24    |
| 13. MN55(N G)MN56C40 | 14. NA23(N G)NA24C40 |
| 15. NI58(N 2N)NI57   | 16. NI58(N P)CO58    |
| 17. NP237(N F)FP*B10 | 18. P31(N P)SI31     |
| 19. PU239(N F)FP*B10 | 20. S32(N P)P32      |
| 21. S34(N HE)SI31    | 22. SI28(N P)AL28    |
| 23. TH232(N F)FP*B10 | 24. TH232(NG)TH233   |
| 25. U235(N F)FP*B10  | 26. U238(N F)FP*B10  |
| 27. U238(N G)U239C40 | 28. ZN64(N P)CU64    |
| 29. ZR90(N 2N)ZR89   |                      |

It is necessary to submit the cross-sections every time to run the RDMM code. Thus, the author applied the CSTAPE program (a preceding program of SAND II code to generate the cross-section information and stored in the disk) to output the cross-section (in milli-barn) with range from 0.1 to 18 Mev in 0.1 Mev increments. The original cross-section range in CSTAPE program is separated into two regions, one by dividing from  $10^{-10}$

to 1 Mev into 10 decades with 45 values in each decade, and the other by dividing the range from 1 to 18 Mev into 0.1 Mev increments.

Figures C.1 to C.4 and Table C are the cross-section information used in RDMM code.



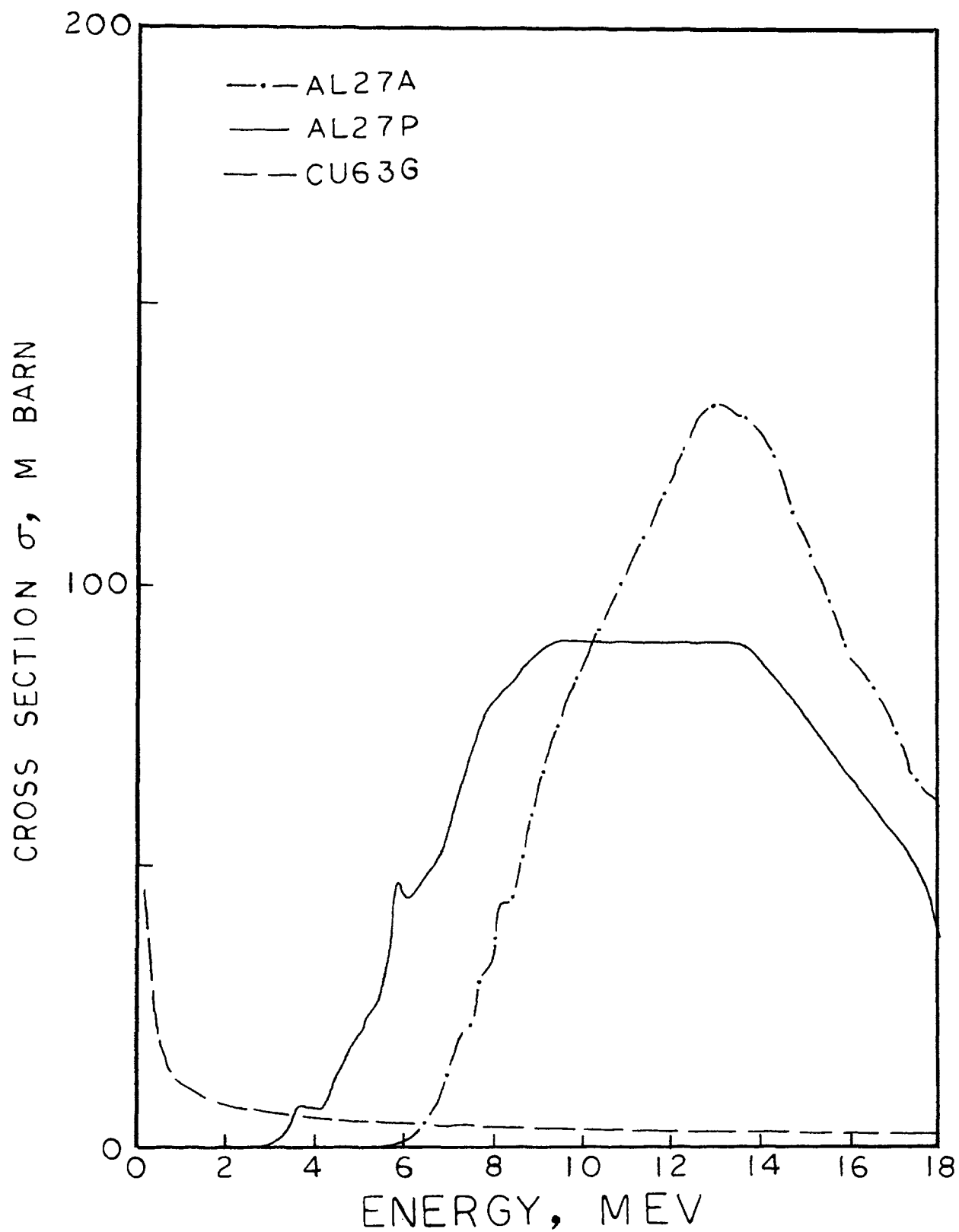


Figure C.1. The cross-section as a function of neutron energy for  $\text{Al}27(n,\text{He})\text{Na}24$ ,  $\text{Al}27(n,p)\text{Mg}27$ ,  $\text{Cu}63(n,g)\text{Cu}64$ .

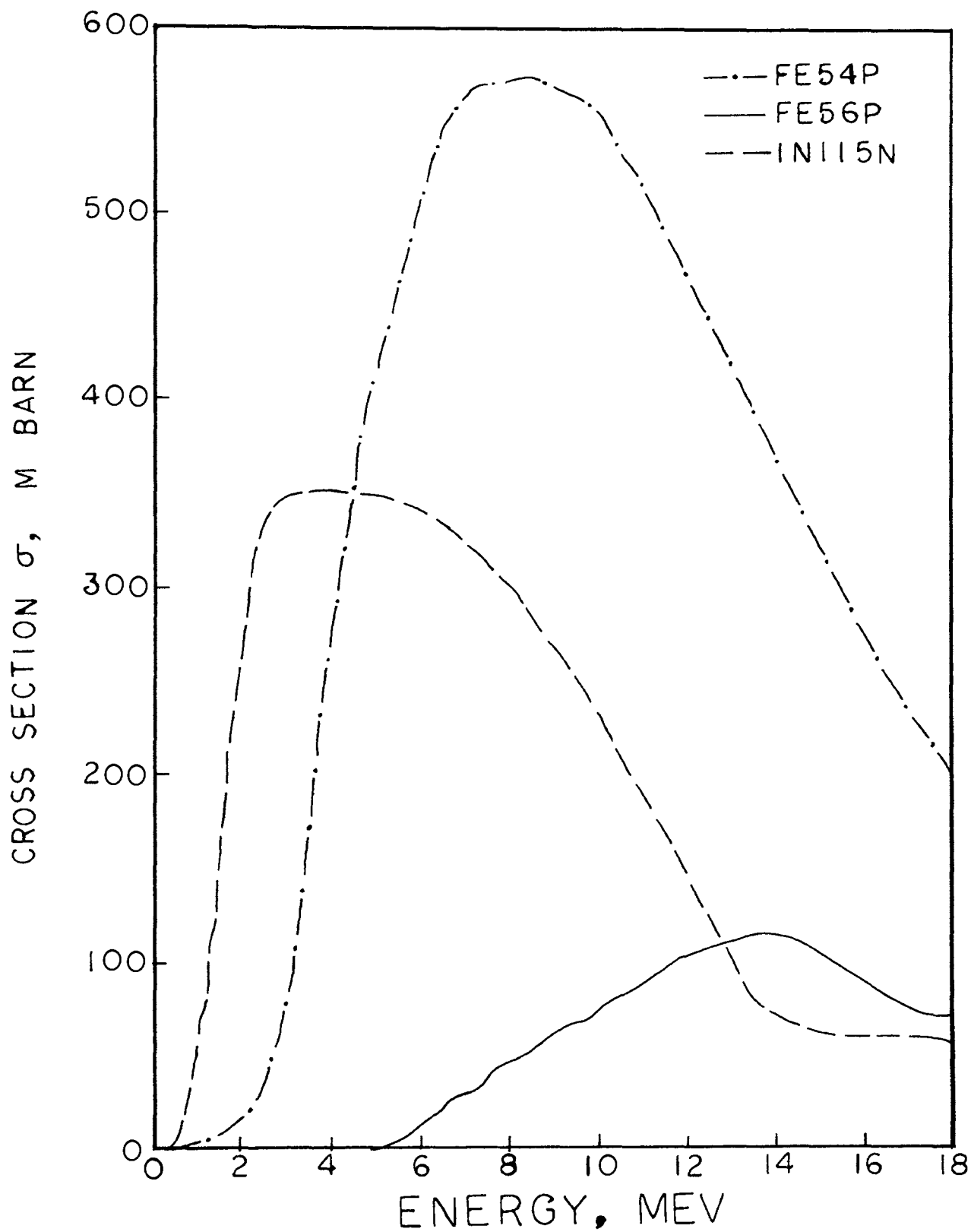


Figure C.2. The cross-section as a function of neutron energy for  $\text{Fe}54(n,p)\text{Mn}54$ ,  $\text{Fe}56(n,p)\text{Mn}56$ ,  $\text{In}115(n,n)\text{In}115m$ .

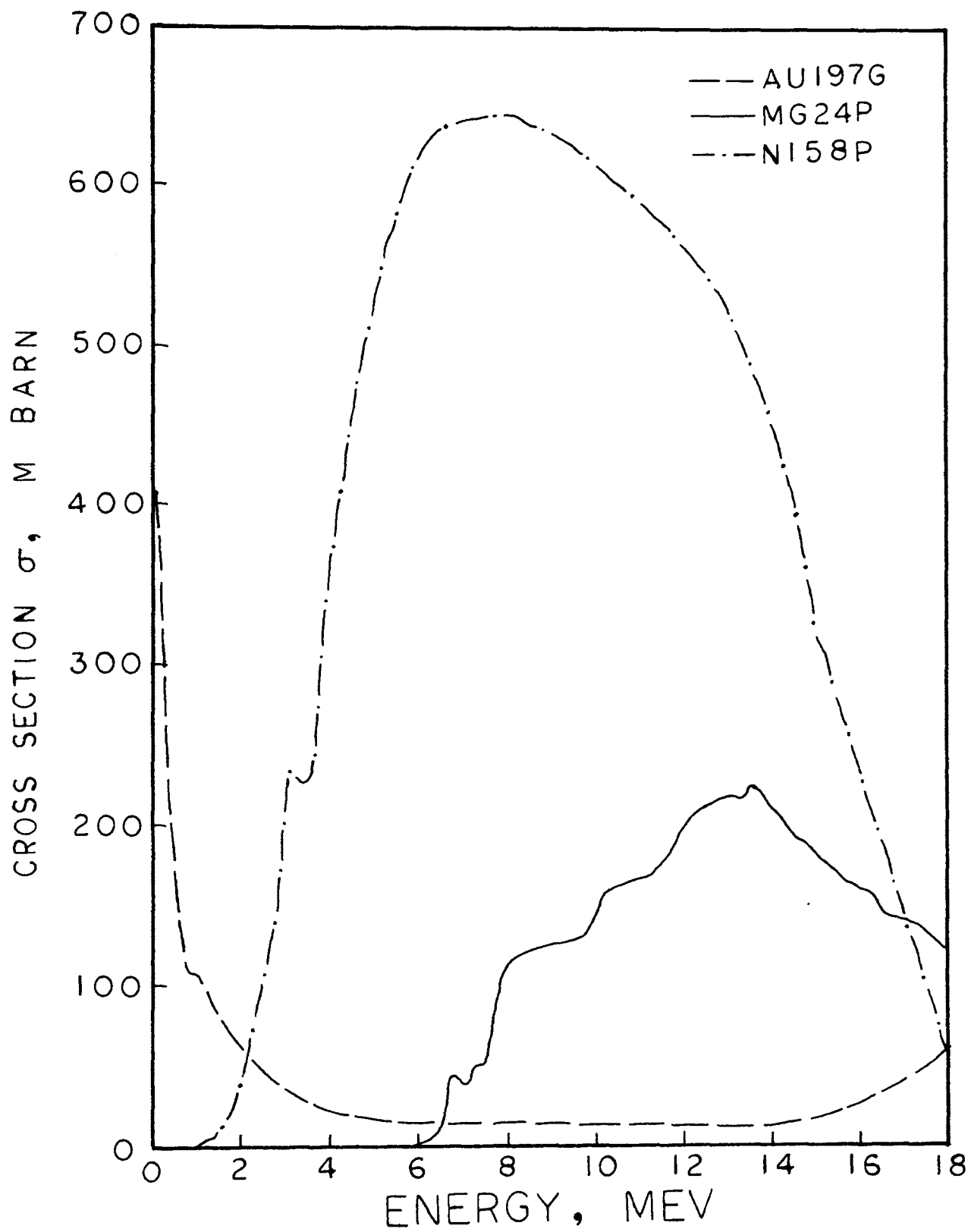


Figure C.3. The cross-section as a function of neutron energy for  $\text{Au}197(n,\text{G})\text{Au}198$ ,  $\text{Mg}24(n,\text{p})\text{Na}24$ ,  $\text{Ni}58(n,\text{p})\text{Co}58$ .

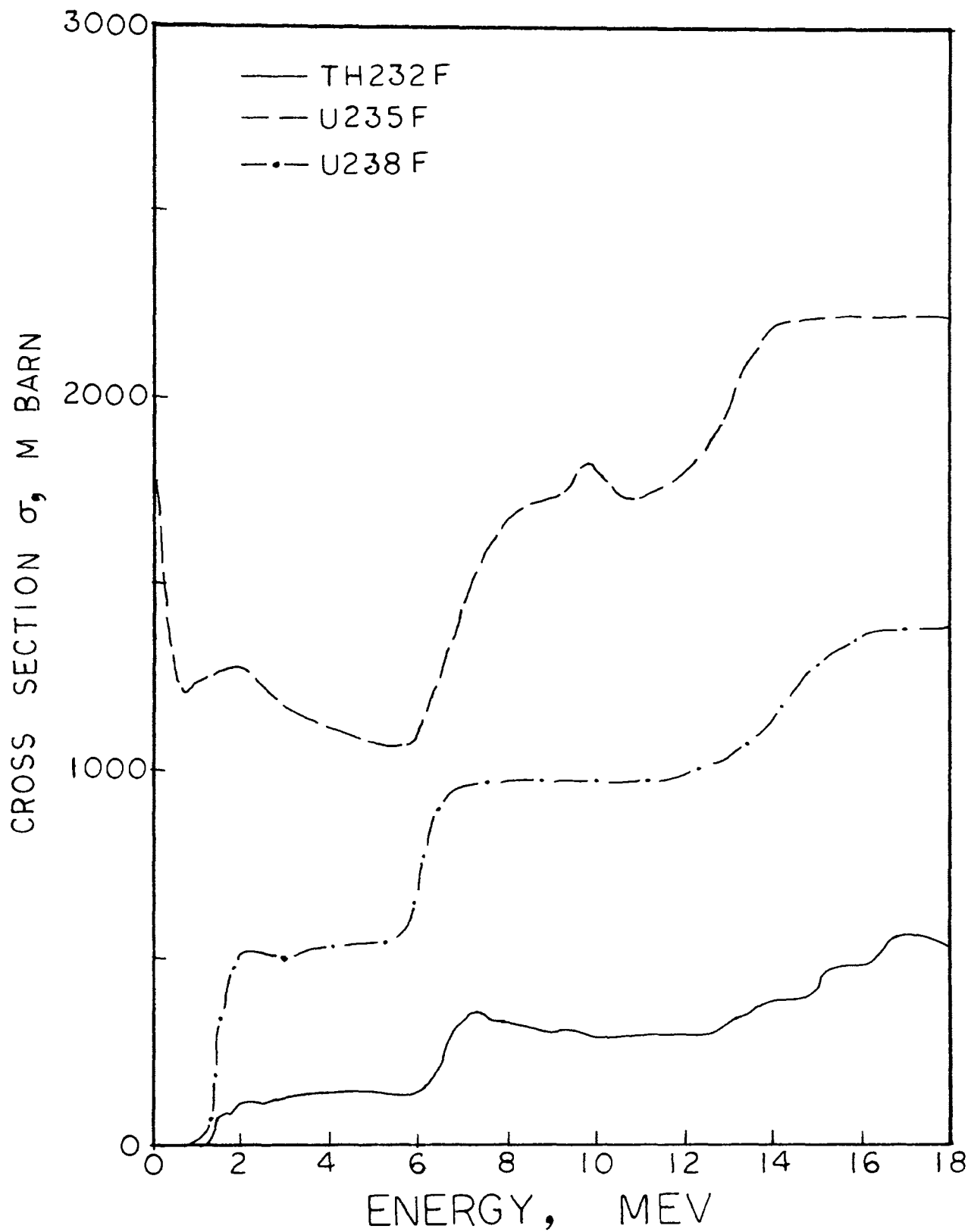


Figure C.4. The cross-section as a function of neutron energy for  $\text{Th}232(n,f)\text{FP}$ ,  $\text{U}235(n,f)\text{FP}$ ,  $\text{U}238(n,f)\text{FP}$ .

Table C. Library Cross-section

1. For Al<sup>27</sup>(n,He)Na<sup>24</sup> as Energy 4.7(.1)18

.003	.014	.034	.055	.074	.093
.117	.154	.233	.378	.578	.831
1.152	1.562	2.093	2.730	3.401	4.238
5.645	7.164	8.346	10.490	13.624	16.014
17.999	20.234	21.175	21.600	24.493	28.963
31.240	31.295	33.558	39.486	43.664	43.341
43.334	45.534	48.293	51.408	54.738	58.118
61.603	64.973	67.894	70.489	72.819	74.844
76.719	78.554	80.404	82.279	84.169	86.064
87.964	89.839	91.589	93.209	94.794	96.384
97.984	99.594	101.249	102.899	104.549	106.199
107.749	109.199	110.600	112.399	114.199	115.899
117.449	119.049	120.899	122.899	124.899	126.899
128.699	130.149	132.249	131.900	132.200	132.350
132.300	132.000	131.451	130.701	130.100	129.850
129.551	128.801	127.701	126.601	125.701	124.751
123.302	121.252	118.753	116.152	113.652	111.202
109.102	107.202	105.202	103.202	101.202	99.257
97.287	95.147	92.952	90.827	88.772	87.016
85.771	84.786	83.826	82.881	81.782	80.362
78.812	77.313	75.848	74.204	72.184	70.014
67.909	65.869	64.228	63.306	62.741	62.201
61.696	30.898				

2. For Al<sup>27</sup>(n,p)Mg<sup>27</sup> as Energy 2.6(.1)18

.075	.225	.400	.600	.897	1.292
1.860	2.600	4.227	6.742	7.750	7.250
6.875	6.625	6.500	6.500	7.874	10.624
12.625	13.875	15.500	17.500	18.975	19.925
21.300	23.100	24.375	25.125	27.349	31.049
36.872	44.822	47.501	44.901	44.057	44.971
45.885	46.840	48.040	49.280	50.520	51.760
53.194	55.800	58.600	61.400	64.200	66.924
69.200	71.400	73.600	75.800	77.824	78.800
79.600	80.400	81.200	82.025	83.000	84.000
85.000	86.000	86.950	87.600	88.200	88.800
89.400	89.925	90.000	90.000	90.000	90.000
90.000	90.000	90.000	90.000	90.000	90.000
90.000	90.000	90.000	90.000	90.000	90.000
90.000	90.000	90.000	90.000	90.000	90.000
90.000	90.000	90.000	90.000	90.000	90.000
90.000	90.000	90.000	90.000	90.000	90.000
90.000	90.000	90.000	90.000	90.000	90.000
90.000	90.000	90.000	90.000	90.000	90.000
90.000	90.000	90.000	90.000	90.000	90.000
90.000	90.000	89.551	88.651	87.751	86.851
85.951	85.051	84.151	83.251	82.351	81.451
80.476	79.426	78.376	77.326	76.276	75.226
74.176	73.126	72.076	71.026	69.976	68.926
67.876	66.826	65.776	64.726	63.676	62.626
61.576	60.526	59.487	58.457	57.427	56.397
55.367	54.337	53.307	52.277	51.247	50.218
48.208	45.208	42.208	39.208	36.209	

## 3. For Au197(n,G)Au198 as Energy .1(.1)18

406.851	339.851	263.001	215.751	179.001	149.001
124.500	110.375	108.500	108.500	105.300	98.900
92.675	87.500	82.500	78.000	74.000	70.000
66.000	62.000	58.500	55.500	52.525	49.700
46.900	44.300	41.900	39.550	37.500	35.500
33.850	32.550	31.250	29.950	28.650	27.450
26.350	25.250	24.150	23.050	22.180	21.540
20.900	20.260	19.620	19.070	18.610	18.150
17.690	17.230	16.800	16.400	16.000	15.600
15.200	14.981	14.944	14.906	14.869	14.831
14.794	14.756	14.719	14.681	14.644	14.606
14.569	14.531	14.494	14.456	14.419	14.381
14.344	14.306	14.269	14.231	14.194	14.156
14.119	14.081	14.044	14.006	13.969	13.931
13.894	13.856	13.819	13.781	13.744	13.706
13.669	13.631	13.594	13.556	13.519	13.481
13.444	13.406	13.369	13.331	13.294	13.256
13.219	13.181	13.144	13.106	13.069	13.031
12.994	12.956	12.919	12.881	12.844	12.806
12.769	12.731	12.694	12.656	12.619	12.581
12.544	12.506	12.469	12.431	12.394	12.356
12.319	12.281	12.244	12.206	12.169	12.131
12.094	12.056	12.019	12.100	12.300	12.500
12.700	12.900	13.200	13.600	14.000	14.400
14.800	15.299	15.899	16.499	17.099	17.699
18.449	19.349	20.249	21.149	22.049	23.049

24.149	25.249	26.349	27.449	28.599	29.799
30.999	32.199	33.398	34.818	36.457	38.097
39.737	41.377	43.076	44.837	46.596	48.356
50.116	52.144	54.444	56.744	59.044	61.344

4. For  $\text{Cu}^{63}(\text{n},\text{g})\text{Cu}^{64}$  as Energy .1(.1)18

45.780	35.663	24.788	19.800	16.725	14.600
13.050	11.975	11.215	10.590	10.103	9.709
9.315	8.921	8.527	8.215	7.985	7.755
7.525	7.295	7.101	6.943	6.785	6.627
6.469	6.330	6.210	6.090	5.970	5.850
5.751	5.672	5.593	5.514	5.435	5.356
5.277	5.198	5.119	5.040	4.973	4.918
4.863	4.808	4.753	4.698	4.674	4.588
4.533	4.478	4.429	4.386	4.344	4.301
4.259	4.216	4.174	4.131	4.089	4.046
4.010	3.981	3.951	3.922	3.892	3.863
3.833	3.804	3.774	3.745	3.718	3.694
3.670	3.646	3.622	3.598	3.574	3.550
3.526	3.502	3.480	3.459	3.428	3.417
3.396	3.375	3.354	3.333	3.312	3.291
3.271	3.253	3.235	3.217	3.199	3.181
3.163	3.145	3.127	3.109	3.094	3.082
3.070	3.058	3.046	3.034	3.022	3.010
2.998	2.986	2.974	2.962	2.950	2.938
2.926	2.914	2.902	2.890	2.878	2.866



2.854	2.842	2.830	2.818	2.806	2.794
2.782	2.770	2.758	2.746	2.734	2.722
2.710	2.698	2.686	2.674	2.662	2.650
2.638	2.626	2.614	2.602	2.590	2.578
2.566	2.554	2.542	2.530	2.518	2.506
2.496	2.489	2.482	2.474	2.467	2.460
2.452	2.445	2.438	2.430	2.423	2.416
2.408	2.401	2.394	2.386	2.379	2.372
2.364	2.357	2.350	2.342	2.335	2.328
2.320	2.313	2.306	2.298	2.291	2.284

5. For Fe54(n,p)Mn54 as Energy .1(.1)18

.177	.271	.454	.636	.818	1.040
1.500	2.012	2.600	3.200	3.900	4.700
5.525	6.500	7.500	8.800	10.400	12.025
13.800	15.600	18.040	21.120	24.455	29.320
34.439	41.199	49.599	58.199	67.999	77.999
91.198	107.597	124.547	144.797	165.596	188.796
214.395	238.810	256.108	272.219	288.330	304.441
320.552	336.663	352.774	368.885	384.116	394.060
403.123	412.185	421.248	430.310	439.373	448.435
457.498	466.560	475.622	484.685	493.747	502.810
511.872	520.934	529.665	536.398	542.798	547.749
551.249	554.749	558.249	561.599	564.799	567.646
568.371	568.741	569.112	569.482	569.852	570.223
570.593	570.963	571.334	571.704	572.075	572.445
572.815	572.426	571.276	570.125	568.975	567.824

566.674	565.523	564.373	563.222	562.072	560.922
559.590	557.732	555.839	553.948	551.053	547.153
543.253	539.353	535.453	531.553	527.653	623.753
519.853	515.953	511.571	506.704	501.837	496.971
492.104	487.237	482.371	477.504	472.637	467.771
462.904	458.037	453.171	448.304	443.438	438.571
433.704	428.838	423.971	419.104	414.238	409.371
404.504	399.638	394.771	389.904	385.038	380.171
375.305	370.438	365.571	360.705	355.838	350.971
346.105	341.238	336.371	331.505	326.638	321.772
316.905	312.038	307.172	302.305	297.439	292.705
288.105	283.505	278.904	274.304	269.904	265.705
261.505	257.306	253.106	249.106	245.306	241.507
237.707	233.908	230.257	226.758	223.258	219.758
216.259	212.759	209.259	205.760	202.260	198.760

6. For Fe<sup>56</sup>(n,p)Mn<sup>56</sup> as Energy 3.6(.1)18

.002	.007	.017	.032	.046	.059
.067	.072	.118	.206	.300	.400
.525	.675	.922	1.267	1.825	2.595
3.510	4.570	5.800	7.200	8.699	10.299
12.128	14.185	16.242	18.310	20.439	22.579
24.719	26.859	28.829	29.780	30.560	31.340
32.120	33.117	35.419	37.939	40.459	42.979
45.297	46.400	47.300	48.200	49.100	50.087
51.599	53.199	54.799	56.399	58.024	59.799

61.599	63.399	65.199	66.849	67.600	68.200
68.800	69.400	70.199	72.199	74.399	76.599
78.799	80.849	81.999	82.999	83.999	84.999
86.049	87.399	88.799	90.199	91.599	93.049
94.799	96.599	98.399	100.199	101.874	102.800
103.599	104.400	105.199	106.999	106.799	107.599
108.349	109.049	109.749	110.449	111.149	111.849
112.549	113.249	113.949	114.650	114.751	114.250
113.751	113.250	112.751	112.251	111.751	111.251
110.751	110.251	109.251	107.751	106.251	104.751
103.252	101.752	100.252	98.752	97.252	95.752
94.252	92.752	91.252	89.752	88.251	86.752
85.252	83.752	82.252	80.752	79.502	78.502
77.502	76.502	75.502	74.502	73.502	72.502
71.502	70.502	70.000	70.000	70.000	70.000
70.000					

7. For In115(n,n')In115m as Energy .4(.1)18

1.062	3.612	8.050	15.275	24.950	38.200
50.500	69.454	76.608	108.937	118.999	159.949
180.869	210.284	229.333	245.985	261.432	283.691
303.999	318.849	326.800	333.600	339.000	342.500
345.000	346.750	348.250	349.300	349.900	350.450
350.700	350.900	351.000	351.000	350.991	350.920
350.840	350.660	350.380	350.100	349.820	349.540
349.260	348.980	348.700	348.420	348.140	347.701

347.101	346.500	345.901	345.301	344.501	343.501
342.476	341.301	340.101	338.731	337.191	335.651
334.111	332.571	330.821	328.861	326.901	324.941
322.981	320.801	318.401	316.001	313.601	311.202
308.809	306.425	304.040	301.655	299.271	296.886
294.336	290.788	287.074	283.360	279.852	276.552
273.252	269.952	266.652	263.202	259.602	256.002
252.402	248.802	245.103	241.303	237.503	233.703
229.903	225.878	221.628	217.378	213.128	208.878
204.628	200.378	196.128	191.878	187.628	183.378
179.128	174.878	170.628	166.378	162.128	157.878
153.628	149.378	145.128	140.704	136.104	131.504
126.904	122.304	117.704	113.104	108.504	103.904
99.304	94.639	89.909	85.180	80.576	77.963
76.201	74.601	73.051	71.801	70.601	69.501
68.501	67.501	66.501	65.501	64.501	63.763
62.938	62.113	61.458	60.972	60.486	60.024
59.700	59.400	59.100	58.800	58.567	58.733
58.967	59.159	59.106	59.013	58.919	58.825
58.731	58.638	58.544	58.450	58.357	58.263
58.169	58.075	57.932	57.643	57.344	57.046
56.747	56.449	56.150			

8. For  $Mg^{24}(n,p)Na^{24}$  as Energy 5.1(.1)18

.013	.029	.035	.043	.055	.078
.125	.258	.936	1.557	2.272	3.484
5.504	8.701	14.522	26.693	42.796	45.200

41.028	37.750	41.546	49.248	51.200	49.800
51.748	70.588	87.569	97.771	106.745	114.498
116.999	118.999	120.500	121.749	123.000	124.000
124.750	125.250	125.750	126.250	126.750	127.250
127.750	128.250	129.000	129.999	131.998	135.248
140.246	148.244	155.747	159.249	160.500	161.500
163.249	164.750	165.500	166.499	167.250	168.000
168.750	169.250	169.750	172.497	176.997	180.748
185.429	191.080	195.431	199.164	202.498	205.831
208.399	210.365	212.475	214.443	216.048	216.667
217.711	219.396	218.656	216.733	216.134	220.996
225.750	224.003	220.670	217.338	214.157	211.080
207.915	204.220	200.436	196.652	193.526	191.760
190.036	187.839	184.950	182.055	179.161	176.289
173.431	170.613	168.402	166.402	164.402	162.568
161.076	159.600	158.770	158.385	157.243	151.538
146.628	144.950	143.641	142.729	141.820	140.911
140.002	139.093	138.086	135.507	132.382	129.258
126.133	123.246	121.803	120.604		

9. For Ni58(n,p)Co58 as Energy 1.1(.1)18

1.336	3.582	5.117	5.430	9.233	11.682
16.437	22.686	29.285	38.721	49.321	62.832
77.349	91.778	104.830	117.407	129.792	145.997
172.496	207.494	232.998	234.002	227.001	227.000
226.501	231.997	257.493	297.491	337.493	364.996
383.746	401.246	419.246	437.746	455.246	471.746

486.997	500.996	513.498	524.497	536.247	548.747
559.747	569.248	578.498	587.497	595.873	603.623
610.623	616.873	621.875	625.624	629.374	633.124
635.750	635.750	638.500	639.500	640.250	640.750
641.375	642.125	642.875	643.625	644.000	644.001
644.001	644.001	644.250	644.750	644.750	644.251
643.001	641.002	639.501	638.501	637.251	635.752
634.500	633.501	632.251	630.751	629.001	627.002
625.002	623.002	620.877	618.627	616.377	614.127
612.002	610.002	607.752	605.252	602.752	600.252
597.977	595.927	593.677	591.227	588.253	584.753
581.753	579.253	577.002	575.002	572.004	568.004
564.503	561.503	558.253	554.753	551.378	548.128
544.628	540.879	536.504	531.505	526.754	522.254
516.506	509.506	503.005	497.006	490.257	482.757
475.257	467.757	460.506	453.507	444.760	434.260
423.760	413.260	401.013	387.013	371.266	353.766
335.019	319.511	309.634	300.884	292.133	283.383
274.633	265.883	257.133	248.383	239.633	230.883
222.084	213.235	204.386	195.537	186.688	177.839
168.989	160.140	151.291	142.442	133.518	124.519
115.520	106.521	97.522	88.522	79.523	70.524
61.525	52.526				

10. For  $\text{Th}^{232}(n,f)\text{FP}$  as Energy 1.2(.1)18

1.720	8.460	38.749	62.005	91.463	92.301
-------	-------	--------	--------	--------	--------

82.184	104.000	112.850	115.623	127.614	124.635
104.475	102.309	116.490	117.313	125.020	127.312
128.493	131.516	130.722	132.475	134.585	135.868
140.841	142.000	141.813	142.417	142.250	142.084
141.589	144.474	144.861	144.500	144.083	144.250
144.417	143.458	143.067	146.184	143.892	143.251
139.876	140.150	136.127	135.584	134.061	135.354
143.250	148.344	163.223	176.639	201.994	229.486
266.486	294.160	311.609	323.746	335.672	351.033
366.999	357.324	352.086	353.998	338.138	326.875
328.813	325.938	326.252	327.723	321.881	321.175
315.255	313.498	314.023	303.683	304.377	300.102
299.198	302.963	311.162	310.014	306.144	306.157
304.941	299.816	294.691	289.566	287.135	287.404
287.673	287.942	288.212	288.481	288.750	289.019
289.289	289.558	289.827	290.096	290.366	290.635
290.904	291.173	291.443	291.712	291.981	292.250
292.519	292.789	293.058	293.327	293.596	293.866
297.266	303.807	310.349	316.890	323.431	329.973
336.514	343.055	349.596	356.138	362.679	369.220
375.762	381.112	382.999	384.666	386.332	387.999
389.666	391.332	392.999	394.666	396.332	404.754
427.153	449.627	464.244	467.899	469.724	471.574
473.099	474.299	475.367	475.632	475.764	475.895
479.800	494.679	510.259	525.839	540.359	544.984
547.192	549.399	551.607	553.814	556.022	558.230

558.591 553.565 548.192 542.820 537.447 532.075  
526.702

11. For U235(n,f)FP as Energy .1(.1)18

1770.883	1620.001	1433.000	1355.500	1282.500	1232.750
1206.250	1202.249	1220.750	1235.500	1246.499	1252.749
1254.250	1256.249	1258.750	1265.499	1273.999	1277.499
1278.000	1276.000	1269.501	1262.000	1252.001	1238.502
1223.501	1209.501	1198.501	1187.501	1177.752	1169.250
1162.001	1156.001	1150.001	1144.001	1138.001	1132.601
1127.800	1123.001	1118.201	1113.401	1108.401	1104.101
1099.501	1094.901	1090.302	1086.001	1082.001	1078.001
1074.001	1070.001	1066.600	1063.800	1061.550	1062.599
1064.198	1065.999	1067.999	1071.647	1085.194	1100.394
1125.386	1160.187	1195.386	1232.985	1270.985	1307.785
1343.386	1379.186	1416.184	1453.384	1485.588	1512.789
1539.339	1561.990	1583.989	1603.692	1621.092	1638.492
1655.892	1673.292	1685.797	1693.398	1700.997	1708.597
1716.197	1721.467	1724.400	1727.332	1730.266	1733.199
1736.132	1739.065	1744.002	1760.989	1779.989	1798.989
1817.989	1832.907	1823.276	1809.543	1795.810	1782.076
1768.343	1754.610	1740.876	1730.505	1723.505	1720.667
1722.498	1727.330	1733.396	1740.195	1746.995	1753.796
1760.596	1768.495	1777.494	1786.494	1795.494	1804.494
1814.867	1826.617	1838.367	1850.116	1864.448	1881.488
1901.733	1925.233	1945.487	1962.487	1995.711	2045.211



2078.113	2094.363	2110.613	2126.863	2143.113	2159.363
2175.611	2191.862	2201.000	2203.000	2205.000	2206.999
2208.999	2210.999	2212.999	2214.999	2216.999	2218.999
2220.001	2220.001	2220.001	2220.001	2220.001	2220.001
2220.001	2220.001	2220.001	2220.001	2220.001	2220.001
2220.001	2220.001	2220.001	2220.001	2220.001	2220.001
2220.001	2220.001	2220.001	2220.001	2220.001	2220.001
2220.001	2220.001	2220.001	2220.001	2220.001	2220.001

12. For U238(n,f)FP as Energy .5(.1)18

.130	.608	1.441	2.411	7.182	15.447
19.735	34.302	46.102	96.561	247.894	341.248
401.248	448.249	481.748	507.250	516.500	518.501
516.001	512.001	509.001	505.001	501.001	498.001
495.501	497.500	502.500	507.000	511.999	516.000
518.500	521.500	524.000	526.000	528.250	530.750
532.750	534.250	535.001	535.001	535.500	536.500
537.750	539.250	540.001	540.001	540.001	540.001
541.250	543.750	549.997	559.997	574.994	599.990
636.485	686.480	753.971	813.985	854.986	887.491
907.495	924.493	939.497	948.998	955.498	959.000
961.499	963.500	964.500	965.001	966.500	968.400
969.201	969.901	970.001	970.001	970.001	970.001
970.001	970.001	970.001	970.001	970.001	970.001
970.001	970.001	970.001	970.001	970.001	970.001
970.001	970.001	970.001	970.001	970.001	970.001

970.001	970.001	970.001	970.001	970.001	970.001
970.001	970.001	970.001	970.001	970.001	973.000
975.000	977.000	979.000	981.000	983.000	985.249
988.998	992.998	996.598	999.798	1003.197	1007.796
1012.596	1016.997	1020.996	1025.246	1030.994	1036.995
1043.993	1051.993	1059.994	1067.993	1075.994	1085.391
1096.190	1106.791	1116.192	1125.392	1140.581	1161.781
1182.533	1200.584	1218.184	1233.788	1247.388	1260.638
1271.790	1282.590	1292.591	1301.791	1310.741	1318.192
1325.393	1332.795	1337.395	1342.995	1348.595	1354.195
1359.196	1363.595	1367.697	1369.998	1371.998	1373.998
1375.998	1377.898	1379.198	1380.398	1381.199	1381.599
1381.999	1382.400	1382.799	1382.801	1382.401	1382.001

## APPENDIX D

## RECOMMENDATIONS IN USING COMPUTER CODES

In order to run the codes reliably and efficiently, several features are recommended as follows:

## D.1 SAND II CODE

1. Name of foils must be the same as the short reaction name in library file. (see Appendix C)
2. Extrapolation forms  
LOW END E is suggested.
3. Auxiliary output  
NO PLOT NO CARDS is suggested.
4. For ITERATION RUN only  
LIMIT 25           and  
SMOOTH 1   are optimal values.

## D.2 RDMM CODE

1. Number of foils no greater than 10.
2. Number of points in which the  $\sigma(E)$  are tabulated  
NP = 180.
3. MIN = 3, MAX = 6 in most cases.
4. Number of Monte Carlo histories for each approximation order NHIH(I) = 100 for each I.
5. E(1) = 0.1, H = 0.1.
6. Scale factor, SCALE = 1.E19;  
Initial random digit, IX = 5.

### D.3 SPECTRA CODE

1. Name of foils must be the same as the reaction name in library file. (see Appendix C)
2. Number of flux values in field 2 of input data 1 no greater than 35 is suggested.
3. Maximum number of iterations in field 5 of card 1, 1,000 - 2,000 are optional.
4.  $E(2)/E(1)$  value no greater than 10 is suggested.
5. It must be begun with heading card RUN, for every case, and ended with last card ENDEND for ceasing execution.

## APPENDIX E

## CURRENTLY OUTPUT DESCRIPTIONS

## E.1 SAND II CODE

The first page is the data echo check.

In the next N+1 pages that follow the results of each iteration are listed, where N is the actually iteration numbers. These contain:

- Foil name, cover name, lower and upper 5 % activity limits, measured to calculated activity ratio, and deviation (%) of measured from calculated activity. One line for one foil;
- Standard deviation (%) of measured activity;
- Average total flux (above 'NORM' Mev).

On the last page, an appropriate message is printed to indicate the reason for cessation of iteration, and the informations of saturated measured and calculated activity are added too.

The iteration process is currently stopped for any of the following occurs:

1. The standard deviation of measured-to-calculated activity ratios is smaller than the value specified on DEVIATION card;
2. The standard deviation becomes stable to within less than 1 % in two successive iterations at a value higher than that specified;

3. The maximum allowed number of iterations (specified on LIMIT card) is reached.

In the next 17 pages that follow the detailed information is printed from energy range  $10^{-10}$  to 18 Mev. (currently 621 intervals) These contain: energy value, absolute differential and integral flux value, normalized to 'NORM' Mev differential and integral flux value, and average energy value. One line for one energy value.

## E.2 RDMM CODE

The first 5 or 6 pages contain:

- The title of the case;
- The coefficients  $b_j$  of the functions  $\psi_k$ ;
- The coefficient  $w_k$  of the weighting function;
- The activity, its relative standard deviations and the cross-section relative standard deviations;
- The 'cut-off' numbers of the series expansion and the number of the Monte Carlo histories required;
- The scale factor;
- The elements of the matrices S defined in formula (17);
- The elements of the matrices  $R^T R$  defined in formula(22);

In the pages that follow the results of the

computation are listed. For each cut-off number 2 or 3 pages are printed. The first 1 or 2 pages contains:

- The elements of matrices  $R^T R$  of that series expansion;
- The list of the numbers

$$\frac{\int \sigma_1 \psi^k dE}{A_1}$$

- The value of the quadratic form  $Q$  (see Eq. 20);
- The value of integral flux above 0.5 Mev;
- The table of the actual value of  $\psi^k(E)$ .

The next page is listed only if a statistical analysis on the results is required. This page contains all the information concerning this analysis on integral and differential neutron flux. This information is the total and mean flux value and their interval, calculated and Monte Carlo flux, absolute and relative standard deviation, and 68 % confidence interval.

### E.3 SPECTRA CODE

The first two or three pages:

- Input deck echo check;
- The names, activities and weight factors of the foils;
- Initial and normalized initial flux, initial and normalized initial calculated activity ratios;
- Elements of the matrix  $C$  defined in Eq. 26;

- The results from subroutine LIMIT contain calculated differential and integral flux, calculated activities.

The next ten pages or more give the results from subroutine REPETE. This subroutine currently prints out the eigenvalues of  $B^{-1}$ , and the energy points first. It prints out results for each of the first 10 iterations, then every fifth iteration up to 100, then every 100th iteration. The results contain the calculated differential and integral flux values, the calculated activities, the calculated to measured activity ratios, the activity error, the root-mean-squared flux difference with respect to the trial.



## APPENDIX F

## CHARACTERISTICS OF THE UMR REACTOR

Type:	Swimming Pool (modified BSR-type)
Core:	Heterogeneous-uranium, aluminum, water
Al/H <sub>2</sub> O Volume Ratio:	0.7 ± .05
Moderator:	Light Water
Reflector:	Light Water and Graphite
Coolant:	Light Water with free convection flow
Biological Shield:	Light Water and Normal Concrete
Critical Mass:	2.7 kg U-235 for Water Reflector
Power Level:	Up to 200 Kw
Average Thermal Flux:	1.6 x 10 <sup>12</sup> n/cm <sup>2</sup> -sec at 200 Kw with an H <sub>2</sub> O reflector.

Tabulated results for differential flux operating at 200 Kw at core position C.3 are listed in Table F. The diagram of UMR Reactor core is shown in Figure F.1. A key to the fuel prefixes is:

- F - Standard Elements
- C - Control Elements
- S - Source Holder.

Figure F.1. Diagram of UMRR Core Loading 31T

A								
B				S				
C			F12	F8	C4			
D		F22	C1	F15	F11	F18	F2	
E		F5	C2	F13	C13	F3	F14	
F		Bare Rabbit	F21	F10	F7	Cd Covered Rabbit		
	1	2	3	4	5	6	7	8

Table F  
 Tabulated Differential Flux at C.3

E	FLUX	E	FLUX	E	FLUX	E	FLUX
0.1	1.35+8	0.2	8.13+7	0.3	6.05+7	0.4	4.92+7
0.5	4.18+7	0.6	3.66+7	0.7	3.26+7	0.8	2.94+7
0.9	2.67+7	1.0	2.45+7	1.1	2.26+7	1.2	2.09+7
1.3	1.94+7	1.4	1.80+7	1.5	1.68+7	1.6	1.56+7
1.7	1.46+7	1.8	1.36+7	1.9	1.27+7	2.0	1.19+7
2.1	1.12+7	2.2	1.04+7	2.3	9.78+6	2.4	9.16+6
2.5	8.58+6	2.6	8.04+6	2.7	7.53+6	2.8	7.05+6
2.9	6.61+6	3.0	6.19+6	3.1	5.80+6	3.2	5.43+6
3.3	5.09+6	3.4	4.77+6	3.5	4.46+6	3.6	4.18+6
3.7	3.91+6	3.8	3.66+6	3.9	3.43+6	4.0	3.21+6
4.1	3.00+6	4.2	2.81+6	4.3	2.63+6	4.4	2.46+6
4.5	2.30+6	4.6	2.15+6	4.7	2.01+6	4.8	1.88+6
4.9	1.76+6	5.0	1.64+6	5.1	1.54+6	5.2	1.44+6
5.3	1.34+6	5.4	1.26+6	5.5	1.17+6	5.6	1.10+6
5.7	1.02+6	5.8	9.56+5	5.9	8.93+5	6.0	8.34+5
6.1	7.79+5	6.2	7.27+5	6.3	6.79+5	6.4	6.34+5
6.5	5.92+5	6.6	5.52+5	6.7	5.15+5	6.8	4.81+5
6.9	4.49+5	7.0	4.19+5	7.1	3.91+5	7.2	3.64+5
7.3	3.40+5	7.4	3.17+5	7.5	2.96+5	7.6	2.76+5
7.7	2.57+5	7.8	2.40+5	7.9	2.24+5	8.0	2.09+5
8.1	1.94+5	8.2	1.81+5	8.3	1.69+5	8.4	1.57+5
8.5	1.47+5	8.6	1.37+5	8.7	1.27+5	8.8	1.19+5
8.9	1.11+5	9.0	1.03+5	9.1	9.61+4	9.2	8.95+4

Table F (continue)  
 Tabulated Differential Flux at C.3

E	FLUX	E	FLUX	E	FLUX	E	FLUX
9.3	83400	9.4	77700	9.5	72400	9.6	67400
9.70	62800	9.8	58500	9.9	54500	10.0	50700
10.1	47200	10.2	44000	10.3	40900	10.4	38100
10.5	35500	10.6	33000	10.7	30800	10.8	28600
10.9	26700	11.0	24800	11.1	23100	11.2	21500
11.3	20000	11.4	18600	11.5	17300	11.6	16100
11.7	15000	11.8	14000	11.9	13000	12.0	12100
12.1	11200	12.2	10500	12.3	9730	12.4	9060
12.5	8420	12.6	7840	12.7	7290	12.8	6780
12.9	6310	13.0	5870	13.1	5460	13.2	5070
13.3	4720	13.4	4390	13.5	4080	13.6	3800
13.7	3530	13.8	3290	13.9	3050	14.0	2840
14.1	2640	14.2	2450	14.3	8170	14.4	7600
14.5	7060	14.6	6570	14.7	6100	14.8	1580
14.9	1470	15.0	1370	15.1	1270	15.2	1180
15.3	1100	15.4	1020	15.5	950	15.6	883
15.7	821	15.8	763	15.9	709	16.0	659
16.1	612	16.2	569	16.3	529	16.4	491
16.5	457	16.6	424	16.7	394	16.8	366
16.9	340	17.0	316	17.1	294	17.2	273
17.3	254	17.4	236	17.5	219	17.6	203
17.7	188	17.8	175	17.9	162	18.0	151

## BIBLIOGRAPHY

1. HUGHES, D. J., (1953), Pile Neutron Research, Addison-Wesley Pub. Co., Cambridge, Mass., Ch. 4.
2. BERG, S., TRW Systems Group, (Aug. 1968), Modification of SAND II, AEC Research & Development Report, BNWL-855.
3. DI COLA, G., TORA, A., (1966), RDMM - A Code for Fast Neutron Spectra Determination by Activation Analysis, EURATOM, Italy, EUR 2985.e.
4. DI COLA, G., ROTA, A., (1965), Calculation of Differential Fast-Neutron Spectra from Threshold-Foil Activation Data by Least-Squares Series Expansion Methods, NS&E: 23, 344-353.
5. GREER, C. R., HALBLEIB, J. A., WALKER, J. V., (1967), SPECTRA - Determination of Neutron Spectra from Activation Measurements, CCC-108 or SC-RR-67-746.
6. GREER, C. R., WALKER, J. V., (1966), A Procedure for the Computation of Neutron Flux from Foil Activation Data - SPECTRA Code, SC-DC-66-1512.
7. TILL, H. A., (1968), Semiempirical Determination of the Differential Fast Flux Spectrum for U-235 Fission with Water Moderator, Masters Thesis, UMR.
8. DIERCKX, R., (1965), Neutron Spectra Measurement in Fast Reactors Using Foils Detectors, EURATOM, Italy, EUR 2532.e.
9. CONTE, S. D., (1965), Elementary Numerical Analysis, McGraw-Hill, Inc., P. 28.

## VITA

Jau Wen Chen was born in Chunghua, Taiwan on November 3, 1944. He graduated from Taiwan Provincial Taichung First High School, Taichung, Taiwan, in July 1963.

October 1964, he entered National Tsing Hua University, Hsinchu, Taiwan. June 1968, he received a Bachelor of Science degree in Nuclear Engineering.

On July 4, 1968, he joined the China Army, and retired from the Army on July 3, 1969.

January 1970, he began study as a graduate student at the University of Missouri - Rolla to pursue the Master of Science degree in Nuclear Engineering. He has held an traineeship from the University of Missouri at Rolla Nuclear Reactor Facility for the period September, 1970 to August, 1971.